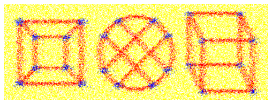
Journal of Graph Algorithms and Applications
http://jgaa.info/ vol. 18, no. 1, pp. 133–173 (2014)
DOI: 10.7155/jgaa.00317

More on Generalized Jewels and the Point Placement Problem [1]

Md. Shafiul Alam [1] *Asish Mukhopadhyay*[1]

[1]School of Computer Science, University of Windsor, 401 Sunset Avenue, Windsor, ON, N9B 3P4, Canada

Abstract

The point placement problem is to determine the positions of a set of n distinct points, $P = \{p_1, p_2, p_3, \ldots, p_n\}$, on a line uniquely, up to translation and reflection, from the fewest possible distance queries between pairs of points. Each distance query corresponds to an edge in a graph, called point placement graph (*ppg*), whose vertex set is P. The uniqueness requirement of the placement translates to line-rigidity of the *ppg*. In this paper we show how to construct in 2 rounds a line-rigid point placement graph of size $4n/3 + O(1)$ from certain small-sized graphs called 6:6 jewels. This improves an earlier result that used cycle-graphs on 5 vertices. More significantly, we improve the lower bound on 2-round algorithms from $17n/16$ to $12n/11$.

Submitted:	Reviewed:	Revised:	Accepted:	Final:
July 2012	February 2013	May 2013	January 2014	February 2014

Published:
February 2014

Article type:
Regular paper

Communicated by:
X. He

Some parts of this paper appeared in CCCG 2009 [2] and CCCG 2010 [1].
This research was supported by an NSERC discovery grant awarded to the second author.
E-mail addresses: alam9@uwindsor.ca (Md. Shafiul Alam) asishm@uwindsor.ca (Asish Mukhopadhyay)

1 Introduction

1.1 The problem

Let $P = \{p_1, p_2, ..., p_n\}$ be a set of n distinct points on a line L. In this paper, we address the problem of determining a unique placement (up to translation and reflection) of the p_i's on L, by querying distances between some pairs of points p_i and p_j, $1 \leq i, j \leq n$.

The resulting queries can be represented by a *point placement graph* (*ppg*, for short), $G = (P, E)$, where each edge e in E joins a pair of points p_i and p_j in P if the distance between these two points on L is known and the length of e, $|e|$, is the distance between the corresponding pair of points (Note the dual use of p_i to denote a point on L as well as a vertex of G).

We will say that G is *line rigid* or just *rigid* when there is a unique placement for P. Thus, the original problem reduces to the construction of a line rigid *ppg*, G.

Let's take some simple examples to illustrate the ideas involved. Suppose we have just 3 points $\{p_1, p_2, p_3\}$ on a line whose positions we want to know. Three different *ppg*s, up to relabelling, are possible (omitting the trivial case when $E = \emptyset$) as shown in Fig. 1 below. Fig. 1(a) corresponds to the situation when the distance between a pair of points, say p_1 and p_2, is known. For Fig. 1(b), the distances between 2 pairs of points, say $\{p_1, p_2\}$ and $\{p_2, p_3\}$, are known. Fig. 1(c) is the *ppg* when all the pairwise distances are known.

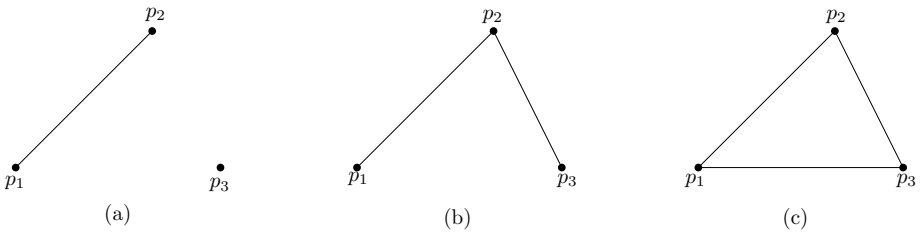

Figure 1: Some point placement graphs for 3 points

Clearly, for the *ppg* of Fig. 1(a) a unique placement is not possible since the point p_3 can be anywhere relative to p_1 and p_2. The same is true of Fig. 1(b) - say we place p_1 and p_2 first, but then the position of p_3 relative to p_2 is ambiguous. However, a unique placement is possible for the *ppg* of Fig. 1(c) as long as the length of one edge is the sum or absolute difference of the lengths of the other two. Thus, if we first place p_1 and then place p_2 to p_1's right, p_3 will be placed between p_1 and p_2 if the sum of its distances from p_1 and p_2 is $|p_1p_2|$, and to the left of p_1 or to the right of p_2 if the absolute difference of the distances is equal to $|p_1p_2|$. In other words, the *ppg* of Fig. 1(c) is rigid.

The last case suggests a simple algorithm for the unique placement of n points. Query the distance between two points, say p_1 and p_2. The position of each of the remaining points p_i, $i \geq 3$ is determined by querying the distances

from p_i to p_1 and p_2; p_i lies between p_1 and p_2 if the sum of the distances is equal to $|p_1p_2|$, and to the left of p_1 or to the right of p_2 if the difference of the distances is equal to $|p_1p_2|$. The corresponding *ppg* shown in Fig. 2 is then rigid. The number of queries made is $2n-3$, which is of the form $\alpha n + \beta$.

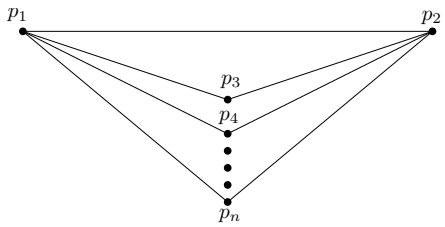

Figure 2: Query graph using triangles

The principal goal is to make α as small as possible. With this in mind, let's look at the more complicated and illuminating case when we have 4 points. Many different *ppg*'s are possible. We can dispense with those that have fewer than 4 edges since in these cases a unique placement is clearly not possible. Fig. 3 below shows the possible *ppg*'s, up to relabelling, with 4 and 5 edges.

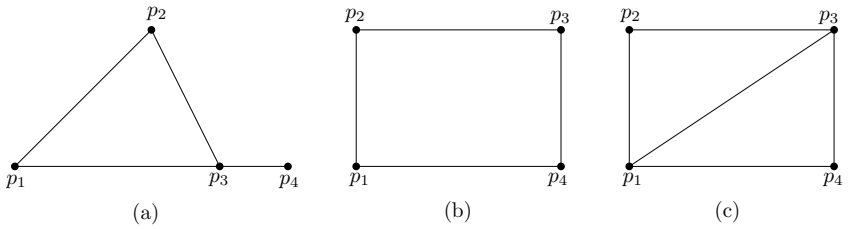

Figure 3: Some point placement graphs for 4 points

The *ppg* of Fig. 3(a) is not rigid, for while the triangle formed by p_1, p_2 and p_3 is rigid, the point p_4 can be placed to the left or right of p_3, making the placement non-unique. The *ppg* of Fig. 3(b) is interesting in that if the two pairs of opposite edges are equal then there is no unique placement. This is easily seen by drawing the *ppg* as a rectangle as shown in Fig. 4(a) below and then giving a horizontal right shear to the top edge p_2p_3 so that p_2 and p_3 lie on the same line as p_1 and p_4, giving us the linear configuration shown in Fig. 4(b). A horizontal left shear produces the linear configuration shown in Fig. 4(c), which cannot be obtained from the linear configuration of Fig. 4(b) by translation and/or reflection.

The *ppg* of Fig. 3(c) is rigid since we have 2 triangles attached to the edge p_1p_3, each of which is rigid. Thus, it is the *ppg* of Fig. 3(b) for which we have a structural rigidity condition, namely, $|p_1p_2| \neq |p_3p_4|$ or $|p_2p_3| \neq |p_1p_4|$ [4]. This means that if we want to extend our previous algorithm for the unique placement of n points, by first placing two nodes, say, p_1 and p_2 on L and then

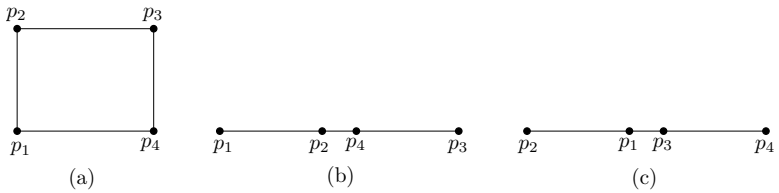

Figure 4: Point placement graph in the shape of a quadrilateral (a) with opposite edges being equal have 2 placements as shown in (b) and (c)

building rigid quadrilaterals by querying distances from p_1 and p_2 with respect to two new nodes at a time, we must make sure that we meet the structural condition on the rigidity of each new quadrilateral.

To build a rigid *ppg* we need to do the queries in rounds. Here is a 2-round algorithm due to Damaschke [6]. Let the number of points be $n = 2b + 4$, where b is a positive integer. In the first round, we make $2b+3$ distance queries represented by the edges in the graph in Fig. 5. There are b children p_i $(i = 3, ..., b+2)$ rooted at p_1 and $b+2$ children p_j $(j = b+3, ..., 2b+4)$ rooted at p_2.

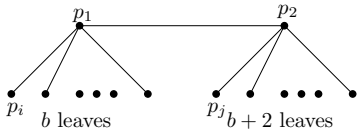

Figure 5: Query graph for first round in a 2-round algorithm using quadrilaterals

In the second round, for each edge p_1p_i $(i = 3, ..., b+2)$ we find an edge p_2p_j rooted at p_2 satisfying the rigidity condition $|p_1p_i| \neq |p_2p_j|$. We can ensure this condition by having 2 extra edges at p_2, in view of the following basic observation [7]:

Observation 1 *At most two equal length edges can be incident to any node in a ppg.*

By Observation 1, there are at most 2 edges p_2p_j such that $|p_1p_i| = |p_2p_j|$. So, for each edge p_1p_i an edge p_2p_j will always be found such that $|p_1p_i| \neq |p_2p_j|$. Then for each i $(i = 3, ..., b + 2)$, we query the distance p_ip_j to form a quadrilateral $p_1p_ip_jp_2$. It will be line rigid since $|p_1p_i| \neq |p_2p_j|$. It will fix the positions of p_i and p_j relative to p_1 and p_2. For each of the 2 unused leaves p_j, the distance p_1p_j is queried in the second round to form the triangle $p_1p_jp_2$. It will fix the position of p_j relative to p_1 and p_2.

The number of queries made over the two rounds to construct this rigid *ppg* is $3b + 5$, i.e., $3n/2 - 1$. There are two noteworthy points: (a) we have reduced the value of α from 2 for the first algorithm to 3/2 for the second, and (b) there is a price for this - we have to query the edges in two rounds.

What if the number of points is greater than 6 but odd? Let $n = 2b + 5$, where b is a positive integer. We make an unique placement of the first $2b + 4$

nodes using the above algorithm, and query the distances of the last odd node from any two nodes. Distance queries for this node can be made in either of the 2 rounds.

1.2 Motivation

The motivation for studying this problem stems from the fact that it arises in diverse areas of research, to wit computational biology, learning theory, computational geometry, etc.

In learning theory [6] this problem is one of learning a set of points on a line non-adaptively, when learning has to proceed based on a fixed set of given distances, or adaptively when learning proceeds in rounds, with the edges queried in one round depending on those queried in the previous rounds.

The version of this problem studied in Computational Geometry is known as the turnpike problem. The description is as follows. On an expressway stretching from town A to town B there are several gas exits; the distances between all pairs of exits are known. The problem is to determine the geometric locations of these exits. This problem was first studied by Skiena *et al.* [11] who proposed a practical heuristic for the reconstruction. A polynomial time algorithm was given by Daurat *et al.* [8].

In computational biology, it appears in the guise of the restriction site mapping problem. Biologists discovered that certain restriction enzymes cleave a DNA sequence at specific sites known as restriction sites. For example, it was discovered by Smith and Wilcox [12] that the restriction enzyme Hind II cleaves DNA sequences at the restriction sites GTGCAC or GTTAAC. In lab experiments, by means of fluorescent in situ hybridization (FISH experiments) biologists are able to measure the lengths of such cleaved DNA strings. Given the distances (measured by the number of intervening nucleotides) between all pairs of restriction sites, the task is to determine the exact locations of the restriction sites.

The turnpike problem and the restriction mapping problem are identical, except for the unit of distance involved; in both of these we seek to fit a set of points to a given set of interpoint distances. As is well-known, the solution may not be unique and the running time is polynomial in the number of points. While the point placement problem, prima facie, bears a resemblance to these two problems it is different in its formulation - we are allowed to make pairwise distance queries among a distinct set of labeled points. It turns out that it is possible to determine a unique placement of the points up to translation and reflection in time that is linear in the number of points.

1.3 Prior work

Early research on this problem was reported in [10, 9]. In this paper, our first principal reference is [6], where it was shown that the jewel (Fig. 8) and $K_{2,3}$ are both line rigid, as also how to build large rigid graphs of density 8/5 (this is an asymptotic measure of the number of edges per node as the number of nodes

go to infinity) out of the jewel. In a subsequent paper, Damaschke [7] proposed a randomized 2-round strategy that needs $(1+o(1))n$ distance queries with high probability and also showed that this is not possible with 2-round deterministic strategies. Our second principal reference is the work of [4] who improved many of the results of [6]. Their principal contributions are the 3-round construction of rigid graphs of density 5/4 from 6-cycles and a lower bound on the number of queries necessary in any 2-round algorithm.

1.4 Our contribution

In this paper, we determine conditions under which generalizations of the jewel, called $m : n$ jewels, remain line rigid. In [2] we showed how to construct in 2 rounds a line rigid *ppg* on n points, using an instance of a 5:5 jewel as the basic component. The number of edges queried during this construction is $10n/7 + O(1)$. In this paper we extend this result to 6:6 jewels, constructing in 2 rounds a line rigid *ppg* with $4n/3 + O(1)$ queries. This improves the result in [4] for constructing a *ppg* of the same size in 2 rounds using 5-cycles. We also improve substantially the lower bound on any 2-round algorithm from $17n/16$ in [4] to $12n/11$.

2 Generalized jewels

The examples described in the Introduction demonstrates well how small *ppg*'s that are inherently rigid or rigid under some structural conditions can be glued together into a large rigid *ppg*. In this section we introduce a novel type of *ppg*, namely an $m : n$ jewel, several copies of which we plan to glue together to form a large rigid *ppg*.

A generic $m : n$ jewel consists of an m-vertex cycle C_1 and another n-vertex cycle C_2 that are joined by a strut going between two vertices Y (of C_1) and Z (of C_2), and hinged at a third common vertex, X (Fig. 6). An instance of an $m : n$ jewel is obtained by the placement of the nodes that describe the cycles C_1 and C_2.

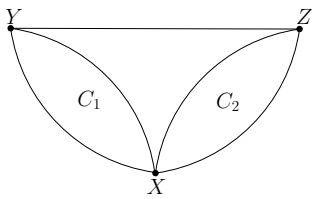

Figure 6: A generic $m : n$ jewel

To attain our goal we need to determine the structural conditions that make a chosen instance of the $m : n$ jewel line rigid. In this, the idea of a layer graph introduced by Chin *et al.* [4] comes in handy. We first choose two orthogonal

directions **x** and **y** (actually, any 2 non-parallel directions will do). A graph G admits a layer graph drawing if the following 4 properties are satisfied:

P1 Each edge e of G is parallel to one of the two orthogonal directions, **x** and **y**.

P2 The length of an edge e is the distance between the corresponding points on L.

P3 Not all edges are along the same direction (thus a layer graph has a two-dimensional extent).

P4 When the layer graph is folded onto a line, by a rotation either to the left or to the right about an edge of the layer graph lying on this line, no two vertices coincide.

Chin *et al.* [4] proved the following result:

Theorem 1 *A ppg G is line rigid iff it cannot be drawn as a layer graph.*

In the next section, we obtain structural conditions under which chosen instances of the $m : n$ jewels remain rigid for small values of m and n by drawing them as layer graphs. Before we do that, we establish a few useful facts about the generic $m : n$ jewel. The first is this.

Theorem 2 *If cycles C_1 and C_2, consisting of m and n nodes respectively, are line rigid then so is any $m : n$ jewel made up of these two cycles.*

Proof: Since C_1 and C_2 are rigid their respective vertices have unique linear layouts. Then in order for an $m : n$ jewel to have a layer graph drawing these placements would have to be in the orthogonal directions **x** and **y**. Suppose the vertex Y is placed on the **x**-axis and the vertex Z on the **y**-axis, then the edge $\overline{YZ}$ of the $m : n$-jewel is not parallel to either the **x** or the **y** direction. Hence, the $m : n$ jewel cannot be drawn as a layer graph and must, therefore, be rigid. □

As a direct consequence of the theorem we have the following corollary:

Corollary 3 *If an $m : n$ jewel has a layer graph representation then in this representation at least one of C_1 or C_2 is a layer graph.*

In order to obtain the structural conditions that make a cycle rigid, we draw all possible layer graph representations of it and find the structural conditions for the rigidity of each of these. The logical AND of all these conditions is our answer. The second corollary is this:

Corollary 4 *The union of the set of all the structural conditions that make C_1 rigid with those that make C_2 rigid, constitute a* sufficient *set of structural conditions that make an $m : n$ jewel rigid.*

We shall take this route in the next two sections to obtain the structural conditions for the rigidity of chosen instances of the $m : n$ jewels for some small values of m and n.

It should be noted that a cycle with a fixed set of n_x **x**-parallel edges and thus a fixed set of n_y **y**-parallel edges can be drawn as a layer graph in different ways. They are all considered to be equivalent. For example, the three layer graph drawings of a 5-cycle in Fig. 7 are considered to be equivalent. From now on, for an equivalent class of layer graphs we shall draw just one of them - not all. We shall not use the term class either. By a particular layer graph, we shall mean the class of layer graphs that are equivalent to it. Thus, two layer graph drawings of an n-vertex cycle are *distinct* from each other if at least one edge has different orientations in the two graphs.

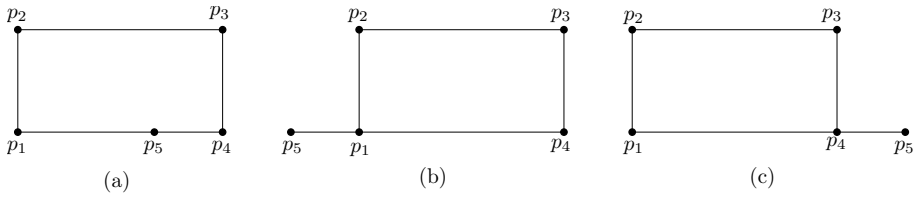

Figure 7: Equivalent layer graphs for a class of layer graphs of a 5-cycle

As we shall resort to exhaustive enumerations of all the layer graph representations of a cycle, the following theorem [2] is useful for checking that we have the correct number.

Theorem 5 *There are* $2^{n-1} - \frac{n^2-n+2}{2}$ *different layer graph representations of an* n*-vertex cycle.*

2.1 4:4 and 5:4 Jewels

The following observation is fundamental. A formal proof can be found in [6].

Observation 2 *A 4-cycle* $XAYB$ *is line rigid if* $|XA| \neq |YB|$ *or* $|XB| \neq |YA|$.

Two 4-cycles joined together as in Fig. 8 is called a jewel in [6]. It is an instance of a generic $4 : 4$ jewel that we will use in the rest of our discussion. To begin with, we prove the following theorem:

Theorem 6 *The 4:4 jewel of Fig. 8 is line rigid.*

Proof: We claim that cycles $XAYB$ and $XQZP$ are both line rigid. Let the edge YZ is **x**-parallel. Three cases arise:

Case 1 The 4-cycle $XAYB$ is line rigid, while the 4-cycle $XQZP$ has a layer graph representation.

Since $XQZP$ is a 4-cycle evidently its layer graph can be a rectangle only. Let the vertices of the line rigid 4-cycle $XAYB$ lie on the **x**-parallel line

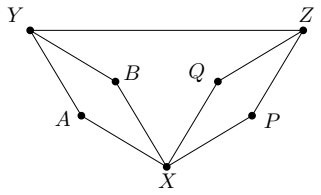

Figure 8: An instance of a 4 : 4 jewel

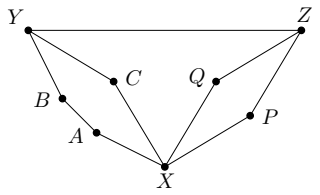

Figure 9: An instance of a 5 : 4 jewel

through Y. Then for the rectangular layer graph $XQZP$ the diagonally opposite vertices X and Z lie on an **x**-parallel line collinear with YZ. Consequently, $XQZP$ cannot have a 2-dimensional extent. This violates property P1 of a layer graph. Thus the 4-cycle $XQZP$ cannot be drawn as a layer graph.

To complete the argument assume that the vertices of the line rigid 4-cycle $XAYB$ lie on the **y**-parallel line through Y. Then the only way we can draw the 4-cycle $XQZP$ as a layer graph such that X and Z are non-adjacent is to place one of the two vertices P or Q at Y. As this violates property P4 that a layer graph should have, the 4-cycle $XQZP$ can not be drawn as a layer graph.

Thus, the 4-cycle $XQZP$ does not have a layer graph representation when the 4-cycle $XAYB$ is line rigid.

Case 2 An identical argument as in Case 1 proves that a layer graph representation of the 4-cycle $XAYB$ is impossible when the 4-cycle $XQZP$ is line rigid.

Case 3 Finally, assume both the 4-cycles have layer graph representations.

Evidently, each of these is a rectangle only. As X and Y are non-adjacent vertices, they are diagonally opposite vertices of the rectangle $XAYB$. Likewise, X and Z are diagonally opposite vertices of the rectangle $XQZP$.

The arguments adduced for Case 1 can once again be used to show that it is not possible to draw the 4-cycle $XAYB$ as a layer graph if X lies on the **x**- or **y**-parallel lines passing through Y or on any of the **x**- or **y**-parallel lines passing through Z.

Assume otherwise. Now, X and Y are diagonally opposite vertices of the rectangle $XAYB$ while X and Z are diagonally opposite vertices of the rectangle $XQZP$. Therefore a vertex of the 4-cycle $XAYB$ must coincide with a vertex of the 4-cycle $XQZP$ on an **x**-parallel line collinear with YZ. As this violates property P4 that a layer graph should have, the cycles $XQZP$ and $XQZP$ cannot have simultaneous layer graph representations.

Thus, none of the two 4-cycles of the jewel has a layer graph representation. By Theorem 1 both the cycles are line rigid, and by Theorem 2 the 4:4 jewel is line rigid. □

Unlike the 4:4 jewel of Fig. 8, the 5:4 jewel of Fig. 9 is not intrinsically line rigid. As a prelude to our discussion in the following sections, it is interesting to find the structural conditions (or simply conditions) that make it line rigid.

We first determine the conditions that make the cycle $XABYC$ line rigid. By Theorem 5, there are five distinct layer graph representations of the 5-cycle $XABYC$, shown in Fig. 10. As remarked earlier, each is a canonical representative of an entire class of layer graph representations; referring to Fig. 10(a) for example, other representations can be obtained by varying the position of A on the supporting line of $\overline{XB}$.

It is impossible to extend the layer graph representations of the 5-cycle $XABYC$ shown in Figs. 10(a) and (b) into a layer graph representation of the entire 5:4 jewel of Fig. 9 without one of the vertices P or Q coinciding with one of the vertices B or C.

However, it is possible to extend each of the layer graph representations of Figs. 10(c)-10(e) into a layer graph representation of our 5:4 jewel. The layer graph representations of Figs. 10(c)-10(e) can be prevented by insisting on the condition $|XC| \neq |AB|, |XA| \neq |YB|, |YC| \neq |AB|$ respectively. By Theorem 1, these collectively constitute a set of sufficient conditions for the line rigidity of the 5-cycle $XABYC$.

For the 4-cycle $XPZQ$ the rigidity condition is $|XP| \neq |ZQ|$ (Observation 2). Thus by Corollary 4, the set of sufficient conditions for the rigidity of the 5:4 jewel of Fig. 9 is $\{|XC| \neq |AB|, |XA| \neq |YB|, |YC| \neq |AB|, |XP| \neq |ZQ|\}$.

We note in passing that for each of the configurations in Figs. 10(c)-10(e), we have an alternate condition that prevents its drawing as shown. Thus for example $|XA| \neq ||CY| \pm |YB||$ also prevents the layer graph drawing of Fig. 10(c). With the help of the label mapping (X, C, Y, B, A) to $(p_3, p_4, p_5, p_1, p_2)$ we can see that this condition encapsulates the 3 different conditions corresponding to the 3 equivalent layer graphs representations shown in Fig. 7. In such situations, whenever possible, we choose the simpler condition, unless the other one is more useful for the construction of a *ppg*.

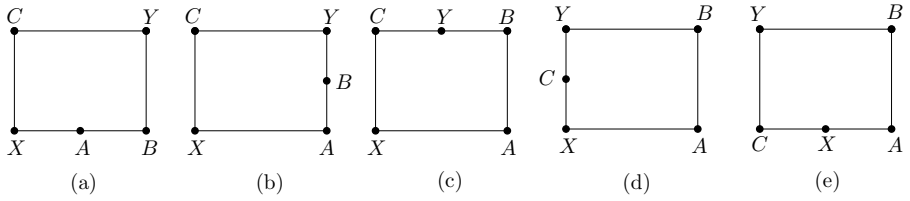

Figure 10: Different layer graph representations of a 5-cycle

Theorem 7 *The 5:4 jewel of Fig. 9 is line rigid if its edges satisfy the set of conditions* $\{|XC| \neq |AB|, |XA| \neq |YB|, |YC| \neq |AB|, |XP| \neq |ZQ|\}$.

3 Algorithm based on a 5:5 jewel

We next consider the more complex case of the 5:5 jewel of Fig. 11. From now on, we will refer to it simply as the 5:5 jewel.

By Theorem 5 there are exactly 5 distinct layer graph representations of a 5-cycle (see Fig. 10). Thus, the set of 5 distinct conditions in Lemma 1 are sufficient to ensure the line-rigidity of the 5-cycle $XABYC$.

Lemma 1 *A 5-cycle $XABYC$ is line rigid if its edges satisfy the following conditions:*

$$|XC| \neq |YB|, |XA| \neq |YC|, |XC| \neq |AB|, |XA| \neq |YB|, |YC| \neq |AB| \quad (1)$$

Proof: Omitted. A formal proof appears in [4]. □

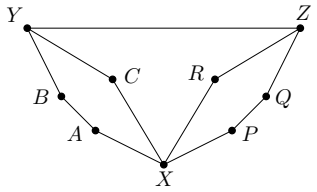

Figure 11: An instance of the 5:5 jewel

For the 5-cycle $XPQZR$ these conditions are:

$$|XR| \neq |ZQ|, |XP| \neq |ZR|, |XR| \neq |PQ|, |ZR| \neq |PQ|, |XP| \neq |ZQ|.$$

By Corollary 4, these 10 conditions collectively constitute a sufficient set of conditions for the line-rigidity of the 5:5 jewel.

Our goal is to glue several copies of the 5:5 jewel of Fig. 11 into a large *ppg*, as we did in the case of quadrilaterals in section 1.1. All of these will have a common strut YZ. As each jewel will account for 7 new nodes in lieu of 10 new edge queries, we expect α to be 10/7. This indeed turns out to be the case. The challenge here is to design the *ppg* in such a way that the rigidity conditions are satisfied for every jewel.

The rigidity conditions for a cycle, in their current form, involve all its edges. This requires to query the lengths of all of its edges in the first round to check if the rigidity conditions are satisfied. This does not provide us with the flexibility of choice that we need to meet the rigidity conditions in a 2-round algorithm. The edge lengths may not satisfy the conditions. If any condition is not satisfied then the cycle and thus the whole jewel may not be line rigid because our set of conditions is sufficient (Theorem 2). Now, the 2-dimensional stretch of a layer graph gives a pointer - we can avoid involving one edge of a cycle from all the rigidity conditions for it. We shall avoid AB and PQ from the rigidity

conditions for the two 5-cycles. Then the cycles will be rigid irrespective of the lengths of those edges. And the rigidity conditions for the cycles will involve all of their other edges. Again, in each rigidity condition we need to have at least one edge in it for which we can choose edge length, from among the options for edge lengths for that particular edge, that satisfies the condition. We shall provide options for choosing each of the edges YB and ZQ.

There will be rigidity conditions of each cycle that will not involve these edges, i.e., YB or ZQ. We cannot meet those rigidity conditions in a 2-round algorithm. We need to avoid other edge(s) from the rigidity conditions of a cycle and/or provide options for choosing edge(s) for a cycle. We shall avoid XC and XR from the rigidity conditions for the two cycles. Then we shall have options for choosing edges YC and ZR to satisfy the rigidity conditions.

Thus, we shall avoid AB, PQ, XC and XR from the rigidity conditions. For each 5-cycle we shall replace each of its rigidity conditions that involve any of these edges. We shall replace that condition by a set of condition(s) that prevent the cycle from being drawn as the layer graph representation that corresponds to that condition.

Looking ahead slightly, Fig. 18 describes the structure of our proposed *ppg*. It has a pool of edges hanging from each end of the strut YZ and a set of 2-pronged subgraphs. The lengths of the edges of this *ppg* are queried in the first round. In the second round, we join each 2-pronged subgraph to a pair of edges incident to Y and another pair of edges incident to Z to form a 5:5 jewel, making sure that all the rigidity conditions satisfied.

Over the rest of this section we show how to replace the rigidity conditions of the 5-cycle $XABYC$ that involve XC and/or AB with rigidity conditions that exclude these edges. To replace a condition we shall find another set of conditions that prevents the drawing of the 5-cycle $XABYC$ as a layer graph in the configuration corresponding to that condition. For example, to replace the condition $|XC| \neq |YB|$, corresponding to the layer graph of Fig. 10(a), we shall find a set of conditions that prevent the drawing of the layer graph of the 5-cycle in the configuration of Fig. 10(a).

Our first attempt will be to use other edges in the layer graph drawing corresponding to a given rigidity condition involving XC and/or AB. If this does not suit our purpose, the basic strategy will be to embed the layer graph drawing corresponding to such a rigidity condition into all possible layer graph drawings of the 5:5 jewel and derive a rigidity condition from each such embedding.

The rigidity conditions that we will consider for replacement are:

$$|XC| \neq |YB|,\ |XC| \neq |AB|,\ |YC| \neq |AB|$$

3.1 Replacing $|XC| \neq |AB|$

This condition has been derived from the layer graph drawing shown in Fig. 10(c). This figure shows that an alternate rigidity condition is

$$|XA| \neq ||YB| \pm |YC||, \tag{2}$$

which we use to replace $|XC| \neq |AB|$.

3.2 Replacing $|XC| \neq |YB|$

This rigidity condition corresponds to the layer graph drawing of Fig. 10(a). $||XA| \pm |AB|| \neq |YC|$ is an alternate rigidity condition corresponding to the layer graph drawing in Fig. 10a) of the 5-cycle $XABYC$. However, it involves the edge AB that we wish to avoid. We shall find an alternate set of rigidity conditions. For this, we find all possible layer graph drawings of the 5:5 jewel in which the layer graph of Fig. 10(a) is embedded. Then we find conditions which prohibit those layer graph drawings. Consequently, those conditions will replace $|XC| \neq |YB|$, because there will be no layer graph for the 5:5 jewel in which the layer graph of Fig. 10(a) is embedded. We shall follow this method whenever we cannot use any rigidity condition for a 5-cycle $XABYC$ or $XPQZR$ that involves some edges of the corresponding cycle only. We have the following lemma for the replacement of the current condition:

Lemma 2 *The 5-cycle $XABYC$ of the 5:5 jewel of Fig. 11 cannot be drawn as the layer graph of Fig. 10(a) if the edges of the jewel satisfy the following conditions:*

$$\{|ZR| \neq |YB|, |ZR| \neq |YC|\} \tag{3}$$

Proof: We argue below that there are exactly 4 possible layer graph drawings of the 5:5 jewel in which the layer graph of Fig. 10(a) lies embedded. Two cases arise depending on the orientations of YZ:

- YZ is horizontal (Fig. 12)

  Z is necessarily distinct from C, while YZ and YB are mutually perpendicular. Consider the edges on the path XRZ of the 5:5 jewel. If XR were vertical, then ZR would have to be horizontal, forcing R to coincide with C. Thus, XR must be horizontal and consequently, RZ must be vertical.

  Next, we consider the edges on the path $XPQZ$. XP can be horizontal or vertical. If XP is horizontal then PQ must be vertical, else Q and R will coincide. This forces QZ to be horizontal giving us the layer graph of Fig. 12(a).

  If XP is vertical, then PQ must be horizontal; otherwise, Q will coincide with C. This forces QZ to be vertical, giving us the layer graph of Fig. 12(b).

  In these layer graphs, the edges YC and YZ are on a horizontal line CYZ, and are parallel to XR. The vertical edges XC and ZR connect the parallel edges. So, we must have $|XC| = |ZR|$. Thus, these layer graphs are not possible if $|ZR| \neq |YB|$.

- YZ is vertical (Fig. 13)

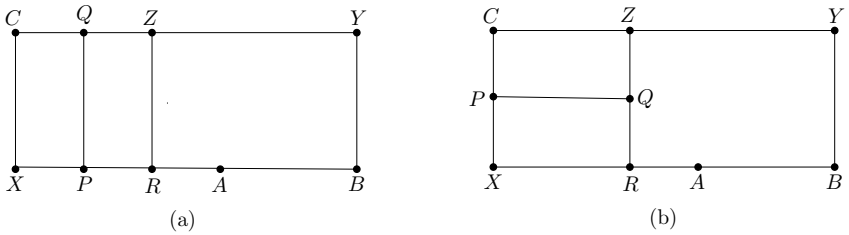

Figure 12: Replacing the condition $|XC| \neq |YB|$ when YB and YZ are mutually perpendicular

Identical arguments as adduced for the case when YZ was assumed horizontal, gives us the layer graph drawings of Fig. 13(a) and Fig. 13(b).

For both the configurations of Fig. 13 the edges XC and XR are on a vertical line XRC, while the edges YB and YZ are on a vertical line BZY. The edge YC is horizontal and connects those two parallel lines. The edge ZR is horizontal and connects the two vertical lines XRC and BZY. So, we must have $|ZR| = |YC|$. Thus, these layer graphs are not possible if $|ZR| \neq |YC|$.

It follows that there is no layer graph for the 5:5 jewel in which the layer graph in Fig. 10(a) of the 5-cycle $XABYC$ is embedded if the edges of the jewel satisfy Eq. 3. Hence, the 5-cycle $XABYC$ of the 5:5 jewel of Fig. 11 cannot be drawn as the layer graph of Fig. 10(a) if the edges of the jewel satisfy the conditions in Eq. 3.

□

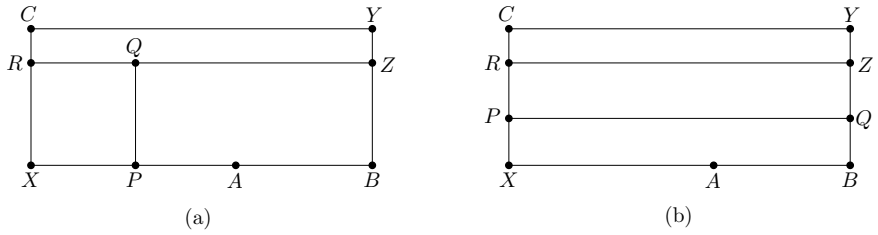

Figure 13: Replacing the condition $|XC| \neq |YB|$ when YB and YZ are collinear

3.3 Replacing $|YC| \neq |AB|$

This rigidity condition corresponds to the layer graph drawing of Fig. 10(e).

We argue below that there are exactly 12 possible layer graph drawings of the 5:5 jewel in which the layer graph of Fig. 10(e) lies embedded. There are 2 main cases to consider.

- YZ is vertical and YB is orthogonal to it:

  The path XRZ is made up of a vertical segment XR, followed by a horizontal segment ZR, else R will coincide with C. If we consider the path XPQ, by a similar argument when XP is horizontal PQ must be vertical. If QZ were vertical, then P would have to coincide with C. Thus, QZ is horizontal. This gives us the layer graph drawing of Fig. 14(a).

  If XP is vertical, we can argue similarly as in the last paragraph that PQ must be horizontal and QZ vertical. This gives us the layer graph drawing of Fig. 14(b).

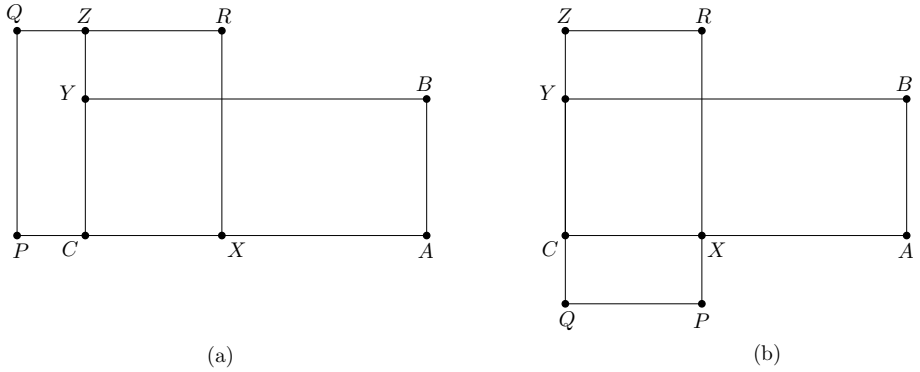

Figure 14: Replacing the condition $|YC| \neq |AB|$ when YZ and YB are perpendicular to each other. There is only one position for R.

$\{|YB| \neq ||XA| \pm |XC||\}$ is an alternate rigidity condition for the 5-cycle $XABYC$ with the layer graph drawing as in (Fig. 10(e)). This condition however involves the edge XC that we wish to avoid. For both the layer graph drawings of Fig. 14, YB and YZ being mutually perpendicular, the edges YC and YZ are on a line CYZ, and they are parallel to XR. So, we must have $|XC| = |ZR|$. Using this, we get the replacement rigidity condition $\{|YB| \neq ||XA| \pm |ZR||\}$.

- YB and YZ are collinear:

  3 subcases arise depending upon the orientations of ZR and XR.

  - ZR is perpendicular to YB and YZ, and XR is perpendicular to ZR (Fig. 15). In this case there are 4 distinct placements of the edges XP, PQ and QZ giving rise to 4 distinct layer graph drawings of the 5:5 jewel (Fig. 15(a)-(d)).

    In all the 4 layer graph drawings the edges YZ and XR are horizontal and collinear, while the edge ZR is vertical and connects those two parallel edges. The edges YB and XA are horizontal and collinear, while the edge AB is vertical and connects those two parallel edges. YZ and YB are collinear, and so are XR and XA. Therefore, we

must have $|AB| = |ZR|$ and the replacement rigidity condition for this subcase is $|YC| \neq |ZR|$.

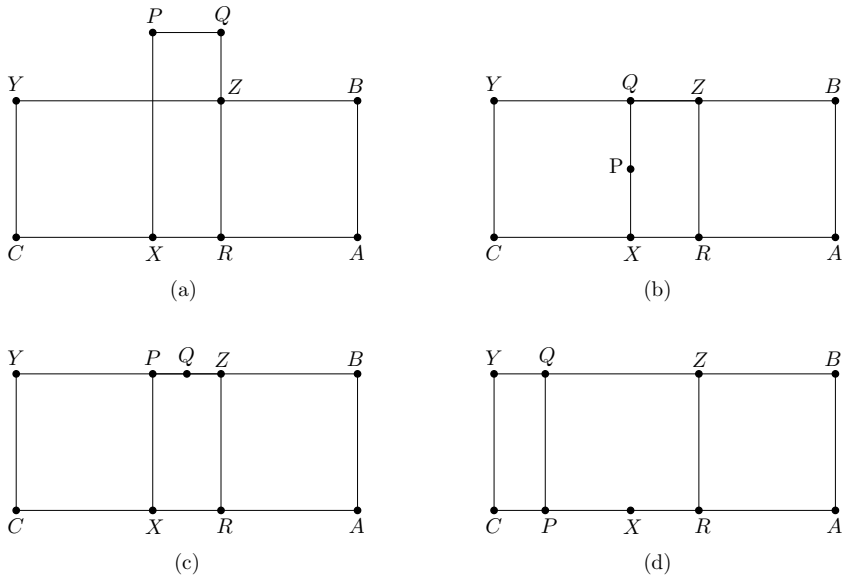

Figure 15: Replacing the condition $|YC| \neq |AB|$ when YB and YZ are collinear, ZR is perpendicular to BYZ and XR is perpendicular to ZR

– ZR is perpendicular to YB and YZ, and XR and ZR are collinear. In this case XP, PQ and QZ can be placed in 2 distinct configurations (Fig. 16). In these configurations of the jewel the 5-cycle $XABYC$ cannot be drawn as a layer graph in the present configuration if $||XA| \pm |XC|| \neq |YB|$. In both the configurations of the layer graph of the jewel YC and XRZ are parallel, and both of XC and YZ connect them. We must have $|XC| = |YZ|$. We can rewrite the condition as $||XA| \pm |YZ|| \neq |YB|$ for this subcase.

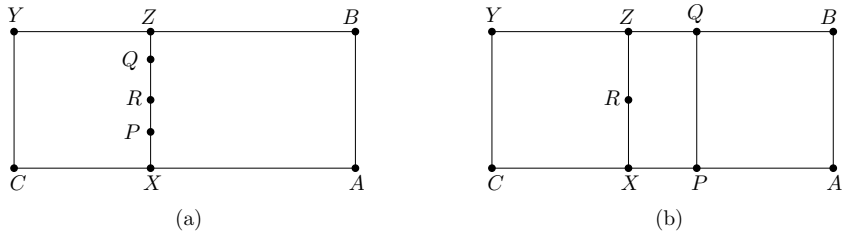

Figure 16: Replacing the condition $|YC| \neq |AB|$ when YB and YZ are collinear, and ZR and XR are perpendicular to BYZ

– ZR is collinear with YB and YZ (Fig. 17). In this case, XR is

necessarily perpendicular to ZR, while XP, PQ and QZ can be in 4 distinct configurations. In all of these, the 5-cycle $XABYC$ cannot be drawn as a layer graph in the present configuration if $||XA| \pm |XC|| \neq |YB|$. Since $|XC| = ||YZ| \pm |ZR||$ in all 4 layer graphs, the condition can be replaced by $||XA| \pm |YZ| \pm |ZR|| \neq |YB|$ for this subcase.

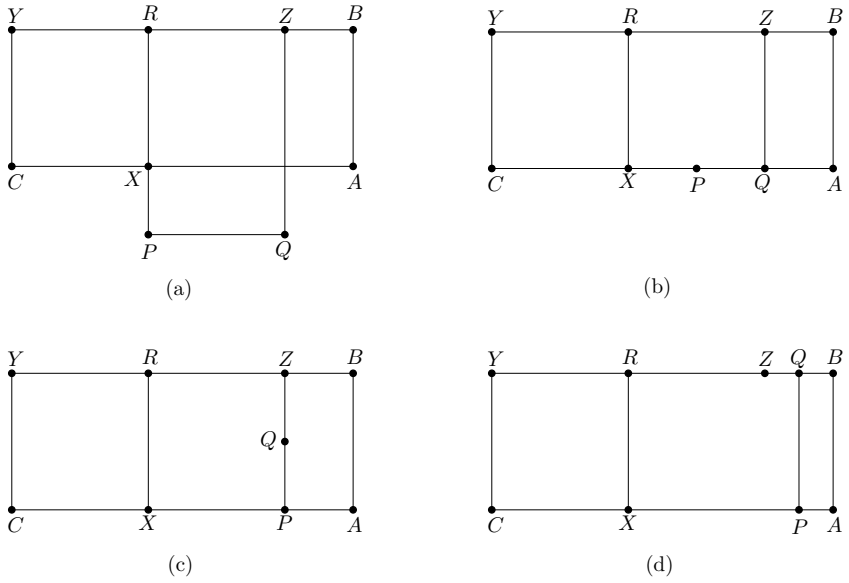

Figure 17: Replacing the condition $|YC| \neq |AB|$ when YB and YZ are collinear and ZR is collinear with them. XR can only be perpendicular to ZR.

Thus, we have the following lemma:

Lemma 3 *The 5-cycle $XABYC$ of the 5:5 jewel of Fig. 11 cannot be drawn as a layer graph in the configuration of Fig. 10(e) if the edges of the jewel satisfy the following conditions:*

$$|YB| \neq ||XA| \pm |ZR||, |YC| \neq |ZR|, ||XA| \pm |YZ|| \neq |YB|, ||XA| \pm |YZ| \pm |ZR|| \neq |YB|.$$

3.4 Rigidity Conditions

From conditions (1)-(2) and Lemmas 2- 3, we have the following result for the line-rigidity of the 5-cycle $XABYC$ of the 5:5 jewel:

Lemma 4 *The 5-cycle $XABYC$ of the 5:5 jewel $XABYCPQZR$ of Fig. 11 is line rigid if the edges of the jewel satisfy the following set of conditions:*

$$\{|ZR| \neq |YB|, |ZR| \neq |YC|, |XA| \neq |YC|, |XA| \neq ||YB| \pm |YC||, |XA| \neq |YB|, |ZR| \neq ||YB| \pm |XA||, |ZR| \neq ||YB| \pm |XA| \pm |YZ||, |YB| \neq ||XA| \pm |YZ||\}.$$

We thus have an amplified set of sufficient conditions to satisfy.

Similarly, we have the following result for the line-rigidity of the other 5-cycle $XPQZR$ of the 5:5 jewel:

Lemma 5 *The 5-cycle $XPQZR$ of the 5:5 jewel $XABYCPQZR$ of Fig. 11 is line rigid if the edges of the jewel satisfy the following set of conditions:*

$$\{|YC| \neq |ZQ|, |YC| \neq |ZR|, |XP| \neq |ZR|, |XP| \neq ||ZQ| \pm |ZR||, |XP| \neq |ZQ|, |YC| \neq ||ZQ| \pm |XP||, |YC| \neq ||ZQ| \pm |XP| \pm |YZ||, |ZQ| \neq ||XP| \pm |YZ||\}.$$

By Corollary 4, the union of the two sets of conditions in Lemmas 4 and 5 constitutes a set of sufficient conditions for the line rigidity of the 5:5 jewel of Fig. 11. Taking care of one overlapping condition between the two sets of 8 conditions, we have 15 distinct conditions for the line-rigidity of the 5:5 jewel and hence the following lemma.

Lemma 6 *The 5:5 jewel $XABYCPQZR$ of Fig. 11 is line rigid if its edges satisfy the following set of conditions:*

1. $|YB| \notin \{|XA|, ||XA| \pm |YZ||\}$,
2. $|YC| \notin \{|XA|, ||YB| \pm |XA||\}$,
3. $|ZQ| \notin \{|XP|, |YC|, ||XP| \pm |YZ||, ||YC| \pm |XP||, ||YC| \pm |XP| \pm |YZ||\}$,
4. $|ZR| \notin \{|XP|, |YB|, |YC|, ||YB| \pm |XA||, ||YB| \pm |XA| \pm |YZ||, ||ZQ| \pm |XP||\}$.

In the next section we show how to construct a composite *ppg* made up of 5:5 jewels such that all the 15 rigidity conditions listed above are satisfied for each of one these.

3.5 Algorithm

We use a pair of points $\{Y, Z\}$ as reference points. We query the edge length $|YZ|$ and the pairwise distances of some other suitable nodes in the first round. All the nodes will be placed relative to Y and Z. Now we consider the second round. We select nodes in groups of 7 nodes each in such a way that the pairwise distances of the union of each group of nodes $\{X, A, B, C, P, Q, R\}$ and $\{Y, Z\}$ satisfy the conditions in Lemma 6. Then we query the remaining necessary pairwise distances of the union to form a 5:5 jewel. The jewel will be line rigid by Lemma 6 irrespective of the lengths of the edges AB, CX, PQ and RX, since no condition of the lemma involves any of these edges. The unused nodes are made line rigid by using triangle as the *ppg*.

Algorithm 1. First a bit of nomenclature. To indicate the affiliations of the vertices X, A, B, C, P, Q, R to different copies of a 5:5 jewel, we use the following indexing scheme: $X \to X_i$, $A \to A_i$, $B \to B_j$, $C \to B_k$, $P \to P_i$, $Q \to Q_m$ and $R \to Q_l$.

Let the number of points be $n = 7b+30$, where b is a positive integer. In the first round, we make $6b + 29$ distance queries represented by the edges in the graph in Fig. 18. There are $2b+6$ children $B_j (j = 1, ..., 2b+6)$ rooted at Y and $2b + 22$ children $Q_l (l = 1, ..., 2b + 22)$ rooted at Z. The remaining $3b$ nodes are organized into groups of 3 as (A_i, X_i, P_i) $(i = 1, ..., b)$ and the distances $|A_iX_i|$ and $|X_iP_i|$, $(i = 1, ..., b)$ are queried.

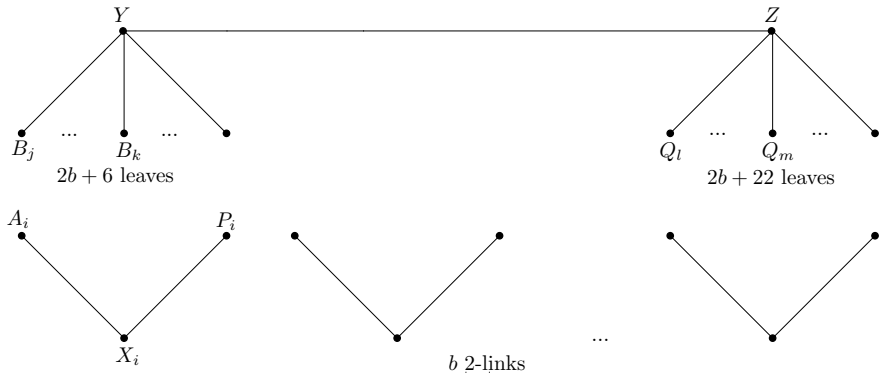

Figure 18: Queries in the first round for a 5:5 jewel

In the second round, for each 2-link (A_iX_i, X_iP_i) we find a pair of edges YB_j and YB_k, rooted at Y satisfying Conditions 1 and 2 of Lemma 6; next, we find a pair of edges ZQ_m and ZQ_l, rooted at Z satisfying Conditions 3 and 4 of Lemma 6.

Then for each $i, (i = 1, ..., b)$, we query the distances $|A_iB_j|$, $|X_iB_k|$, $|X_iQ_l|$ and $|P_iQ_m|$ to form a 5:5 jewel $X_iA_iB_jYB_kP_iQ_mZQ_l$. Its edges will satisfy all the rigidity conditions of Lemma 6.

For each of the 6 unused leaves B_j of the tree rooted at Y, we query the distance $|B_jZ|$ to form the triangle YB_jZ. Likewise, for each of the 22 unused leaves Q_l of the tree rooted at Z we query the distance $|Q_lY|$ to form the triangle YQ_lZ. □

The following theorem establishes the correctness of our algorithm.

Theorem 8 *The ppg constructed by Algorithm 1 is line rigid.*

Proof: Consider an arbitrary 2-link (P_iX_i, X_iA_i). We show that the 5:5 jewel constructed by Algorithm 1 using the edges of this 2-link is line rigid.

Consider the selection of the edge YB_j for the jewel in the second round. From Condition 1 of Lemma 6, $|YB_j|$ cannot be equal to $|X_iA_i|$, $||X_iA_i|+|YZ||$ or $||X_iA_i| - |YZ||$. By Observation 1 there can be at most 2 edges rooted at Y that are equal to a given length. Hence there are at most 6 edges rooted at Y that do not qualify to be chosen as YB_j. By adding 6 extra leaves at Y we provide the room needed to choose YB_j for each of the 2-links (P_iX_i, X_iA_i) with $i = 1, ..., b$, so that the rigidity conditions on this edge are satisfied.

An identical argument shows that the 6 additional leaves at Y enables us to choose YB_k in the second round so that the rigidity conditions on this edge are satisfied for each of the 2-links (P_iX_i, X_iA_i) with $i = 1, ..., b$.

Consider next the selection of the edge ZQ_m for the jewel in the second round. From Condition 3 of Lemma 6, $|ZQ_m|$ cannot be equal to $|X_iP_i|$, $|YB_k|$, $|X_iP_i| + |YZ|$, $||X_iP_i| - |YZ||$, $|YB_k| + |YZ|$, $||YB_k| - |YZ||$, $|X_iP_i| + |YB_k| + |YZ|$, $||X_iP_i| - |YB_k| + |YZ||$, $||X_iP_i| + |YB_k| - |YZ||$, $||X_iP_i| - |YB_k| - |YZ||$. Again from Observation 1 it follows that there are at most 20 edges rooted at Y that do not qualify to be chosen as ZQ_m. Adding 22 extra leaves at Z provides us with the room needed to choose ZQ_m for each of the 2-links (P_iX_i, X_iA_i) with $i = 1, ..., b$, so that the rigidity conditions on this edge are satisfied.

There will be at most 20 edges ZQ_m rooted at Z that do not satisfy the conditions on it as stated in Lemma 6 (Observation 1). In addition to the $2b$ edges necessary to construct the b jewels there are 22 extra edges rooted at Z. So, for each set of 2-link (P_iX_i, X_iA_i) and 3-link (B_jY, B_kY, YZ) with $i = 1, ..., b$ (B_jY depends on P_iX_i and X_iA_i, and B_kY depends on P_iX_i, X_iA_i and B_jY), we can always find an edge YQ_m that satisfies the condition on it as stated in Lemma 6.

Finally, consider the second-round selection of the edge ZQ_l for the jewel. From Condition 4 of Lemma 6 there are 11 rigidity conditions on $|ZQ_l|$, and hence by Observation 1, there will be at most 22 edges ZQ_l rooted at Z that are not eligible to be chosen. In addition to the $2b$ edges necessary to construct the b jewels there are 22 extra edges rooted at Z. So, for each set of 2-link (P_iX_i, X_iA_i) and 4-link (B_jY, B_kY, YZ, ZQ_m) with $i = 1, ..., b$, the 22 extra edges rooted at Z provide us with the latitude to always find an edge ZQ_l that satisfies the rigidity conditions on it.

So, for each 2-link (A_iX_i, X_iP_i) we can always find edges YB_j, YB_k, ZQ_l and ZQ_m for the 5:5 jewel of Fig. 11 such that the conditions for rigidity (Lemma 6) are satisfied. Each of the b 5:5 jewels of Fig. 11 with YZ as an edge is constructed in the second round by satisfying the rigidity conditions of Lemma 6. So, they are line rigid and, for each $i, (i = 1, ..., b)$, the positions of $X_i, A_i, B_j, B_k, P_i, Q_m$ and Q_l are fixed relative to Y and Z. Each of the remaining 6 leaves of Y forms a triangle (YB_j, B_jZ, ZY) with YZ as an edge. So, their positions are fixed relative to Y and Z. Each of the remaining 22 leaves of Z forms a triangle (ZQ_l, Q_lY, YZ) with YZ as an edge. So, their positions are fixed relative to Y and Z.

Hence, the whole *ppg* is line rigid. □

Theorem 9 $10n/7 + 99/7$ *queries are sufficient to place* n *distinct points on a line in two rounds.*

Proof: We need $6b + 29$ queries in the first round and $4b + 28$ queries in the second round. In total $10b + 57$ pairwise distances are to be queried for the placement of $7b+30$ points. We have $10b+57 = 10/7*(7b+30) - 300/7+57 = 10n/7 + 99/7$. □

It is worth noting that our algorithm needs at least 37 points to work. When we have fewer points we can switch to the quadrilateral algorithm, described in the Introduction. The 2-round 5-cycle algorithm of Chin *et al.* [4] a total of $4/3n + 34/3\sqrt{n}$ queries for the placement of n points. Thus, our 5:5 jewel algorithm does better when $n \leq 4076$. This provides the motivation for considering 6:6 jewels, which we do next.

4 Algorithm based on a $6:6$ jewel

The principal ideas underlying this algorithm are similar to the algorithm based on 5:5 jewel of the last section. So we will skip the repetitive details when there is no scope for confusion.

Fig. 19 shows the *ppg* for an instance of the 6:6 jewel that we shall use in the construction of our composite *ppg*. For brevity we will refer to left cycle as C_1 and the right cycle as C_2, and by 6:6 jewel we will mean the instance shown.

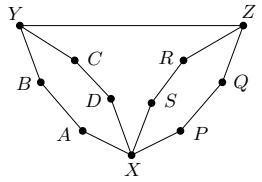

Figure 19: A $6:6$ jewel

By Theorem 5, the 6-cycle $XABYCD$ has 16 different layer graph representations (Fig. 20), giving us the following 16 conditions for its line-rigidity,

$$|YC| \neq |XD|, |YB| \neq |CD|, |YC| \neq |AB|, |YB| \neq |XA|, |XD| \neq |AB|,$$
$$|XA| \neq |CD|, |YB| \neq |XD|, |AB| \neq |CD|, |YC| \neq |XA|, |YB| \neq ||YC| \pm |XD||,$$
$$|YC| \neq ||XA| \pm |XD||, |YB| \neq ||XD| \pm |CD||, |YB| \neq ||XA| \pm |XD||,$$
$$|YB| \neq ||YC| \pm |XA||, |XA| \neq ||YC| \pm |CD||, |XA| \neq ||YB| \pm |CD||. \quad (4)$$

Similarly, we have another set of 16 conditions for the line-rigidity of the cycle C_2, viz.,

$$|ZR| \neq |XS|, |ZQ| \neq |RS|, |ZR| \neq |PQ|, |ZQ| \neq |XP|, |XS| \neq |PQ|, |XP| \neq$$
$$|SR|, |ZQ| \neq |XS|, |ZR| \neq |XP|, |PQ| \neq |RS|, |ZQ| \neq ||ZR| \pm |XS||, |ZR| \neq$$

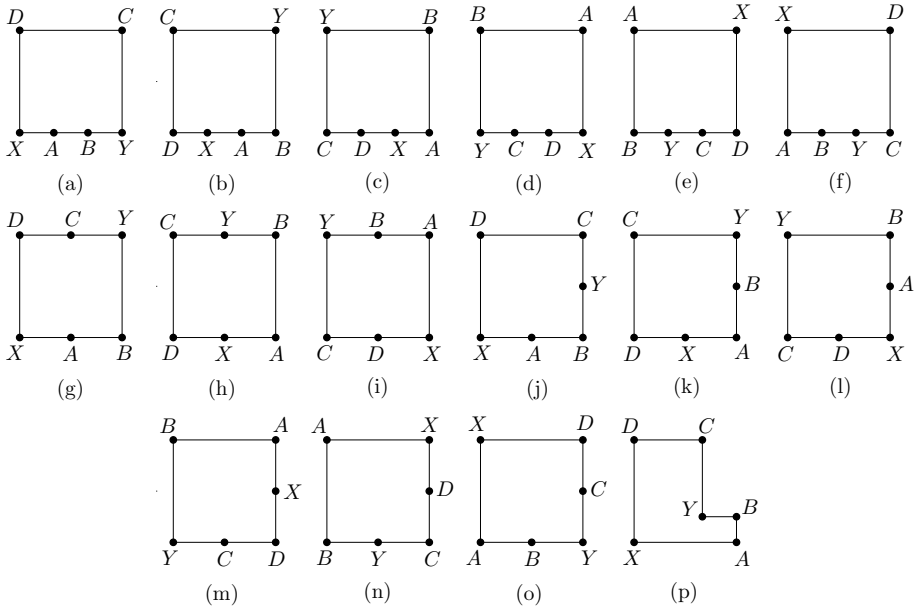

Figure 20: Different layer graph representation of a 6-cycle

$$||XP| \pm |XS||, |ZQ| \neq ||XS| \pm |RS||, |ZQ| \neq ||XP| \pm |XS||, |ZQ| \neq$$
$$||ZR| \pm |XP||, |XP| \neq ||ZR| \pm |RS||, |XP| \neq ||ZQ| \pm |RS||.$$

By Corollary 4, the conjunction of these two sets of conditions constitutes a set of sufficient conditions for the line-rigidity of the 6:6 jewel above.

4.1 Finding substitutes

We would like to make the 6:6 jewel line rigid irrespective of the lengths of the edges AB, CD, PQ and RS as this allows us to query the remaining edges in such a way that the rigidity conditions are satisfied. Towards this goal, we reformulate 16 conditions (8 from each cycle) involving these edges with alternate sets of conditions, satisfying which we also satisfy the replaced ones.

We use the left cycle, $C_1 = XABYCD$, as a running example to demonstrate these replacements.

4.1.1 Replacing $|AB| \neq |CD|$

The layer graph for the 6-cycle C_1 corresponding to this condition is shown in Fig. 20(h). From the figure it is evident that we can replace this with the condition

$$||YB| \pm |YC|| \neq ||XA| \pm |XD|| \tag{5}$$

since this will also prevent the layer graph drawing of the cycle as in Fig. 20(h).

4.1.2 Replacing $|XA| \neq |CD|$

The layer graph of C_1 corresponding to this condition is shown in Fig. 20(f). To replace this condition we follow a similar strategy as for the 5:5 jewel, except for a small twist: we draw all possible layer graphs of the 6:6 jewel, excluding the chain $XSRZ$, in which the layer graph of Fig. 20(f) is embedded. The condition $|XA| \neq |CD|$ is then amplified into the set of conditions that prevent the drawing of the layer graph representation of the 6-cycle corresponding to this condition (Fig. 20(f)). Two cases arise, depending on whether YZ is horizontal or vertical.

- YZ is horizontal:

  Here Z and X have different x and y coordinates. XP, PQ and QZ can have 4 different orientations as shown in Figs. 21(a) - 21(d). The following conditions will prevent the layer graph drawings of the 6-cycle $XABYCD$ in Fig. 20(f), when YZ is horizontal:

  $|ZQ| \neq ||XA| \pm |XP||$ (Fig. 21(a)),
  $||YC| \pm |YZ|| \neq ||XD| \pm |XP||$ (Fig. 21(b)),
  $|ZQ| \neq |XA|$ (Fig. 21(c)) and
  $||ZQ| \pm |YC| \pm |YZ|| \neq ||XD| \pm |XP||$ (Fig. 21(d)).

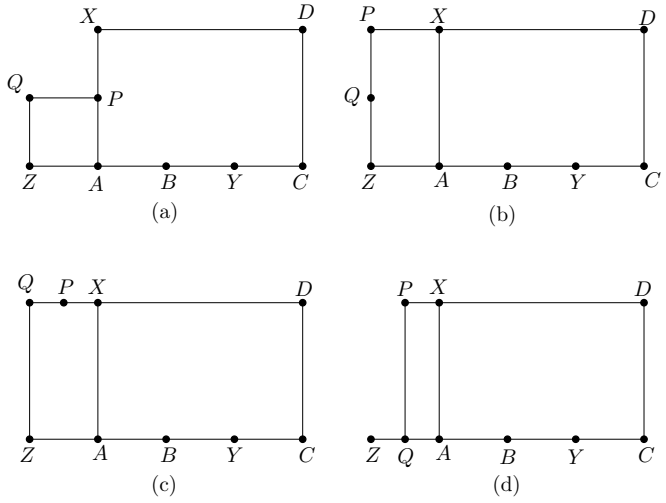

Figure 21: Replacing condition $|XA| \neq |CD|$ when YZ is horizontal

- YZ is vertical and $|YZ| = |XA|$:

  In this case only one layer graph is possible as shown in Fig. 22. We can replace $|XA| \neq |CD|$ with $|YZ| \neq |XA|$. This will prevent the layer graph drawing of the 6-cycle $XABYCD$ in Fig. 20(f) when YZ is vertical and $|YZ| = |XA|$.

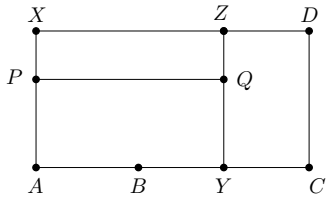

Figure 22: Replacing condition $|XA| \neq |CD|$ when YZ is vertical and $|YZ| = |XA|$

- YZ is vertical and $|YZ| \neq |XA|$:

  Here Z and X have different x and y coordinates. XP, PQ and QZ can have 6 different orientations as shown in Fig. 23(a) - 23(f). These layer graphs give rise to the following set of conditions that prevents the layer graph drawing of the 6-cycle $XABYCD$ as in Fig. 20(f), when YZ is vertical and $|YZ| \neq |XA|$:

  $||ZQ| \pm |YZ|| \neq |XA|$ (Fig. 23(a)), $|YC| \neq ||XD| \pm |XP||$ (Fig. 23(b)),

  $||ZQ| \pm |YZ|| \neq ||XA| \pm |XP||$ (Fig. 23(c)), $||ZQ| \pm |YC|| \neq ||XD| \pm |XP||$ (Fig. 23(d)),

  $||ZQ| \pm |YC|| \neq |XD|$ (Fig. 23(e)) and $|YZ| \neq ||XA| \pm |XP||$ (Fig. 23(f)).

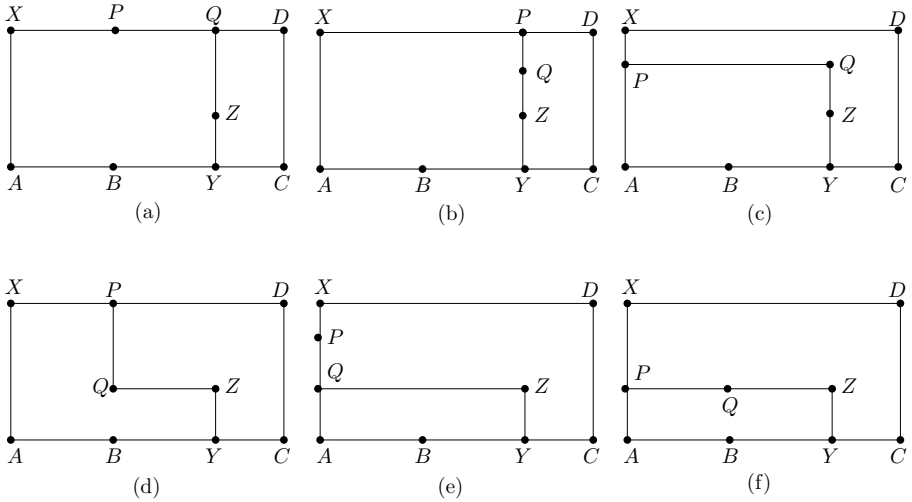

Figure 23: Replacing condition $|XA| \neq |CD|$ when YZ is vertical and $|YZ| \neq |XA|$

Thus, we have the following lemma:

Lemma 7 *The 6-cycle $XABYCD$ of the 6:6 jewel of Fig. 19 cannot be drawn as a layer graph in the configuration of Fig. 20(f) if the edges of the jewel satisfy the following conditions:*

$$|ZQ| \neq ||XA| \pm |XP||, ||YC| \pm |YZ|| \neq ||XD| \pm |XP||, |ZQ| \neq |XA|, ||ZQ| \pm |YC| \pm |YZ|| \neq ||XD| \pm |XP||,$$
$$|YZ| \neq |XA|, ||ZQ| \pm |YZ|| \neq |XA|, |YC| \neq ||XD| \pm |XP||,$$
$$||ZQ| \pm |YZ|| \neq ||XA| \pm |XP||, ||ZQ| \pm |YC|| \neq ||XD| \pm |XP||, ||ZQ| \pm |YC|| \neq |XD|, |YZ| \neq ||XA| \pm |XP||.$$

4.1.3 Replacing $|XD| \neq |AB|$

The layer graph of the 6-cycle corresponding to this condition is as shown in Fig. 20(e). This layer graph is the same as that in Fig. 20(f) if we interchange A with D and B with C. By this interchange of the labels in Lemma 7 we have the following lemma for the replacement of condition:

Lemma 8 *The 6-cycle $XABYCD$ of the 6:6 jewel of Fig. 19 cannot be drawn as a layer graph in the configuration of Fig. 20(e) if the edges of the jewel satisfy the following conditions:*

$$|ZQ| \neq ||XD| \pm |XP||, |YB| \neq ||YZ| \pm |XA| \pm |XP||, |ZQ| \neq ||YB| \pm |YZ| \pm |XA| \pm |XP||, |ZQ| \neq |XD|,$$
$$|YZ| \neq |XD|, |ZQ| \neq ||YZ| \pm |XD| \pm |XP||, |ZQ| \neq ||YB| \pm |XA||,$$
$$|YZ| \neq ||XD| \pm |XP||, |ZQ| \neq ||YB| \pm |XA| \pm |XP||, |ZQ| \neq ||YZ| \pm |XD||, |YB| \neq ||XA| \pm |XP||.$$

4.1.4 Replacing $|YC| \neq |AB|$

The layer graph of the 6-cycle corresponding to this condition is as shown in Fig. 20(c). Fig. 24 shows all the possible layer graphs of the 6:6 jewel, excluding the chain $XSRZ$, in which the layer graph of Fig. 20(c) is embedded (different configurations for P and Q are combined in the same figure).

From Fig. 24 we see that the condition $|YC| \neq |AB|$ can be replaced by the following conditions:

$|ZQ| \neq ||YC| \pm |XP||$, $|ZQ| \neq ||YB| \pm |YZ| \pm |XA||$, $|YC| \neq |XP|$, $|ZQ| \neq ||YB| \pm |YZ| \pm |XA| \pm |XP||$, $|ZQ| \neq |YC|$, $|YB| \neq ||YZ| \pm |XA| \pm |XP||$ (Fig. 24(a)),

$|YB| \neq ||YZ| \pm |XA||$ (Fig. 24(b)),

$|ZQ| \neq ||YB| \pm |XA||$, $|YC| \neq ||YZ| \pm |XP||$, $|ZQ| \neq ||YC| \pm |YZ| \pm |XP||$, $|ZQ| \neq ||YB| \pm |XA| \pm |XP||$ (Fig. 24(c)).

Thus, we have the following lemma:

Lemma 9 *The 6-cycle $XABYCD$ of the 6:6 jewel of Fig. 19 cannot be drawn as a layer graph in the configuration of Fig. 20(c) if the edges of the jewel satisfy the following conditions:*

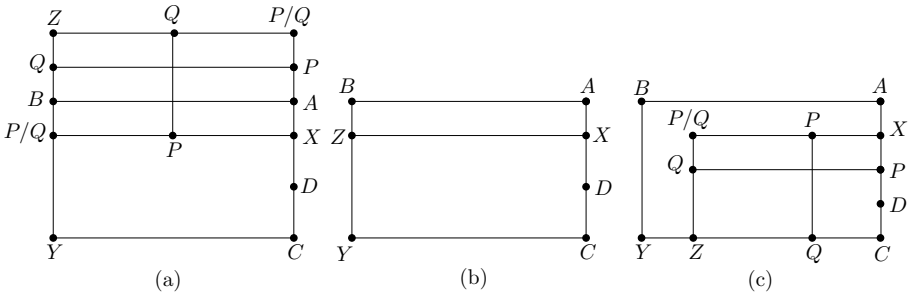

Figure 24: Replacing condition $|YC| \neq |AB|$

$$|ZQ| \neq ||YC| \pm |XP||,\ |ZQ| \neq ||YB| \pm |YZ| \pm |XA||,\ |YC| \neq |XP|,$$
$$|ZQ| \neq ||YB| \pm |YZ| \pm |XA| \pm |XP||,$$
$$|ZQ| \neq |YC|,\ |YB| \neq ||YZ| \pm |XA| \pm |XP||,\ |YB| \neq ||YZ| \pm |XA||,$$
$$|ZQ| \neq ||YB| \pm |XA||,$$
$$|YC| \neq ||YZ| \pm |XP||,\ |ZQ| \neq ||YC| \pm |YZ| \pm |XP||,$$
$$|ZQ| \neq ||YB| \pm |XA| \pm |XP||.$$

4.1.5 Replacing $|YB| \neq |CD|$

The layer graph of the 6-cycle corresponding to this condition is as shown in Fig. 20(b). This layer graph is the same as that in Fig. 20(c) if we interchange A with D and B with C. By this interchange of the labels in Lemma 9 we have the following lemma for the replacement of this condition:

Lemma 10 *The 6-cycle $XABYCD$ of the 6:6 jewel of Fig. 19 cannot be drawn as a layer graph in the configuration of Fig. 20(b) if the edges of the jewel satisfy the following conditions:*

$$|ZQ| \neq ||YB| \pm |XP||,\ |ZQ| \neq ||YC| \pm |YZ| \pm |XD||,\ |YB| \neq |XP|,$$
$$|ZQ| \neq ||YC| \pm |YZ| \pm |XD| \pm |XP||,\ |ZQ| \neq |YB|,$$
$$|YC| \neq ||YZ| \pm |XD| \pm |XP||,\ |YC| \neq ||YZ| \pm |XD||,\ |ZQ| \neq ||YC| \pm |XD||,$$
$$|YB| \neq ||YZ| \pm |XP||,\ |ZQ| \neq ||YB| \pm |YZ| \pm |XP||,$$
$$|ZQ| \neq ||YC| \pm |XD| \pm |XP||.$$

4.1.6 Replacing $|YC| \neq ||XA| \pm |CD||$

The layer graph of the 6-cycle corresponding to this condition is as shown in Fig. 20(o). Fig. 25 shows all the possible layer graphs of the 6:6 jewel, excluding the chain $XSRZ$, in which the layer graph of Fig. 20(o) is embedded.

From Fig. 25 we see that the condition $|YC| \neq ||XA| \pm |CD||$ can be replaced by the following conditions:

$|ZQ| \neq ||YZ| \pm |XD| \pm |XP||$, $|ZQ| \neq |XA|$, $|YZ| \neq ||XD| \pm |XP||$, $|ZQ| \neq ||XA| \pm |XP||$ (Fig. 25(a)),

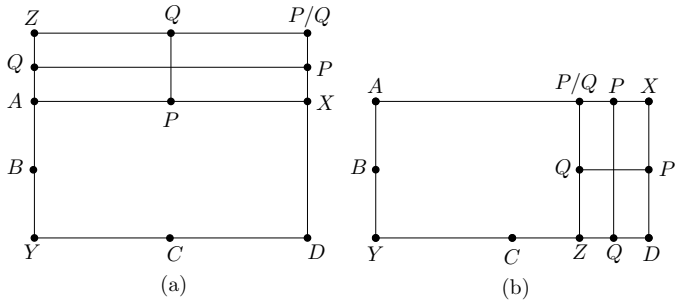

Figure 25: Replacing condition $|YC| \neq |XA| \pm |CD|$

$|ZQ| \neq ||YZ| \pm |XA| \pm |XP||$, $|ZQ| \neq |XD|$, $|YZ| \neq ||XA| \pm |XP||$, $|ZQ| \neq ||XD| \pm |XP||$ (Fig. 25(b)).

Thus, we have the following lemma:

Lemma 11 *The 6-cycle $XABYCD$ of the 6:6 jewel of Fig. 19 cannot be drawn as a layer graph in the configuration of Fig. 20(o) if the edges of the jewel satisfy the following conditions:*

$$|ZQ| \neq ||YZ| \pm |XD| \pm |XP||,\ |ZQ| \neq |XA|,\ |YZ| \neq ||XD| \pm |XP||,$$
$$|ZQ| \neq ||XA| \pm |XP||,$$
$$|ZQ| \neq ||YZ| \pm |XA| \pm |XP||,\ |ZQ| \neq |XD|,\ |YZ| \neq ||XA| \pm |XP||,$$
$$|ZQ| \neq ||XD| \pm |XP||.$$

4.1.7 Replacing $|YB| \neq ||XD| \pm |CD||$

The layer graph of the 6-cycle corresponding to this condition is as shown in Fig. 20(l). Fig. 26 shows all the possible layer graphs of the 6:6 jewel, excluding the chain $XSRZ$, in which the layer graph of Fig. 20(l) is embedded.

From Fig. 26 we see that the condition $|YB| \neq ||XD| \pm |CD||$ can be replaced by the following conditions:

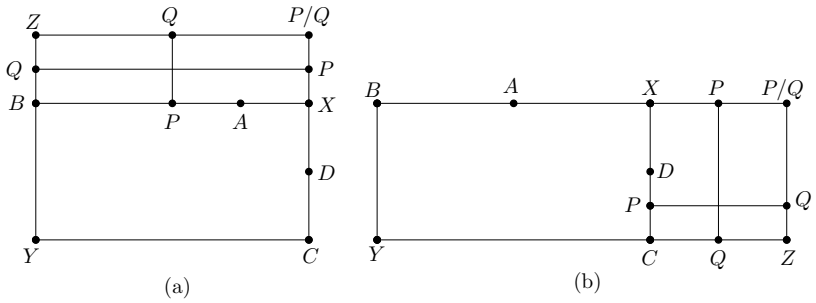

Figure 26: Replacing condition $|YB| \neq |XD| \pm |CD|$

$|ZQ| \neq ||YB| \pm |YZ| \pm |XP||$, $|ZQ| \neq |YC|$, $|YB| \neq ||YZ| \pm |XP||$, $|ZQ| \neq ||YC| \pm |XP||$ (Fig. 26(a)),

$|ZQ| \neq ||YC| \pm |YZ| \pm |XP||$, $|ZQ| \neq |YB|$, $|YC| \neq ||YZ| \pm |XP||$, $|ZQ| \neq ||YB| \pm |XP||$ (Fig. 26(b)).

Thus, we have the following lemma:

Lemma 12 *The 6-cycle $XABYCD$ of the 6:6 jewel of Fig. 19 cannot be drawn as a layer graph in the configuration of Fig. 20(l) if the edges of the jewel satisfy the following conditions:*

$$|ZQ| \neq ||YB| \pm |YZ| \pm |XP||,\ |ZQ| \neq |YC|,\ |YB| \neq ||YZ| \pm |XP||,\ |ZQ| \neq ||YC| \pm |XP||,$$
$$|ZQ| \neq ||YC| \pm |YZ| \pm |XP||,\ |ZQ| \neq |YB|,\ |YC| \neq ||YZ| \pm |XP||,\ |ZQ| \neq ||YB| \pm |XP||.$$

4.1.8 Replacing $|YB| \neq ||XA| \pm |CD||$

The layer graph of the 6-cycle corresponding to this condition is as shown in Fig. 20(p). Fig. 27 shows all the possible layer graphs of the 6:6 jewel, excluding the chain $XSRZ$, in which the layer graph of Fig. 20(p) is embedded.

From Fig. 27 we see that the condition $|YB| \neq ||XA| \pm |CD||$ can be replaced by the following conditions:

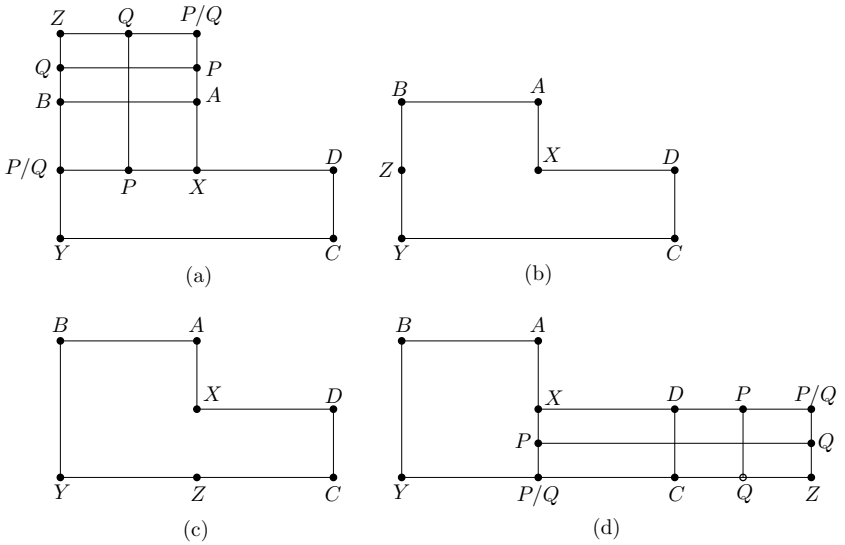

Figure 27: Replacing condition $|YB| \neq |XA| \pm |CD|$

$|ZQ| \neq ||YC| \pm |XD| \pm |XP||$, $|ZQ| \neq ||YB| \pm |YZ| \pm |XA||$, $|YC| \neq ||XD| \pm |XP||$, $|ZQ| \neq ||YB| \pm |YZ| \pm |XA| \pm |XP||$, $|ZQ| \neq ||YC| \pm |XD||$, $|YB| \neq ||YZ| \pm |XA| \pm |XP||$ (Fig. 27(a)),

$|YB| \neq ||YZ| \pm |XA||$ (Fig. 27(b)),
$|YC| \neq ||YZ| \pm |XD||$ (Fig. 27(c)),
$|YB| \neq ||XA| \pm |XP||$, $|ZQ| \neq ||YC| \pm |XD||$, $|ZQ| \neq ||YB| \pm |XA| \pm |XP||$, $|ZQ| \neq ||YB| \pm |XA||$, $|YC| \neq ||YZ| \pm |XD| \pm |XP||$, $|ZQ| \neq ||YC| \pm |YZ| \pm |XD| \pm |XP||$ (Fig. 27(d)).

Thus, we have the following lemma:

Lemma 13 *The 6-cycle $XABYCD$ of the 6:6 jewel of Fig. 19 cannot be drawn as a layer graph in the configuration of Fig. 20(p) if the edges of the jewel satisfy the following conditions:*

$$|ZQ| \neq ||YC| \pm |XD| \pm |XP||,\ |ZQ| \neq ||YB| \pm |YZ| \pm |XA||,$$
$$|YC| \neq ||XD| \pm |XP||,\ |ZQ| \neq ||YB| \pm |YZ| \pm |XA| \pm |XP||,$$
$$|ZQ| \neq ||YC| \pm |XD||,\ |YB| \neq ||YZ| \pm |XA| \pm |XP||,\ |YB| \neq ||YZ| \pm |XA||,$$
$$|YC| \neq ||YZ| \pm |XD||,\ |YB| \neq ||XA| \pm |XP||,\ |ZQ| \neq ||YC| \pm |XD||,$$
$$|ZQ| \neq ||YB| \pm |XA| \pm |XP||,\ |ZQ| \neq ||YB| \pm |XA||,$$
$$|YC| \neq ||YZ| \pm |XD| \pm |XP||,\ |ZQ| \neq ||YC| \pm |YZ| \pm |XD| \pm |XP||.$$

4.2 Rigidity Conditions

From conditions (4)-(5) and Lemmas 7- 13 we have the following lemma for the line-rigidity of the 6-cycle $XABYCD$ of the 6:6 jewel of Fig. 19:

Lemma 14 *The 6-cycle $XABYCD$ of the 6:6 jewel $XABYCDPQZRS$ of Fig. 19 is line rigid if the edges of the jewel satisfy the following conditions:*

$|YZ| \notin$ $\{|XA|, |XD|, ||XA| \pm |XP||, ||XD| \pm |XP||\}$,

$|YB| \notin$ $\{|XA|, |XD|, |XP|, ||XA| \pm |XD||, ||XA| \pm |XP||, ||XA| \pm |YZ||, ||XP| \pm |YZ||, ||XA| \pm |XP| \pm |YZ||\}$,

$|ZQ| \notin$ $\{|XA|, |XD|, |YB|, ||XA| \pm |XP||, ||XD| \pm |XP||, ||XA| \pm |YZ||, ||YB| \pm |XA||, ||XD| \pm |YZ||, ||YB| \pm |XP||, ||XA| \pm |XP| \pm |YZ||, ||XD| \pm |XP| \pm |YZ||, ||YB| \pm |XA| \pm |XP||, ||YB| \pm |XA| \pm |YZ||, ||YB| \pm |XP| \pm |YZ||, ||YB| \pm |XA| \pm |XP| \pm |YZ||\}$,

$|YC| \notin$ $\{|XD|, |XA|, |XP|, |ZQ|, ||ZQ| \pm |XD||, ||ZQ| \pm |XP||, ||YB| \pm |XA||, ||YB| \pm |XD||, ||XA| \pm |XD||, ||XD| \pm |XP||, ||XD| \pm |YZ||, ||XP| \pm |YZ||, ||XD| \pm |XP| \pm |YZ||, ||ZQ| \pm |XD| \pm |XP||, ||ZQ| \pm |XD| \pm |YZ||, ||ZQ| \pm |XP| \pm |YZ||, ||ZQ| \pm |XD| \pm |XP| \pm |YZ||\}$.

Similarly, we have the following lemma for the line-rigidity of the other 6-cycle $XPQZRS$ of the 6:6 jewel:

Lemma 15 *The 6-cycle $XPQZRS$ of the 6:6 jewel $XABYCDPQZRS$ of Fig. 19 is line rigid if the edges of the jewel satisfy the following conditions:*

$|YZ| \notin \{|XP|, |XS|, ||XA| \pm |XP||, ||XA| \pm |XS||\}$,

$|YB| \notin \{|XP|, |XS|, ||XA| \pm |XP||, ||XP| \pm |YZ||, ||XS| \pm |YZ||, ||XA| \pm |XS||, ||XA| \pm |XP| \pm |YZ||, ||XA| \pm |XS| \pm |YZ||\}$,

$|ZQ| \notin \{|XA|, |XS|, |YB|, |XP|, ||XA| \pm |XP||, ||XA| \pm |YZ||, ||YB| \pm |XA||, ||YB| \pm |XP||, ||XP| \pm |XS||, ||XP| \pm |YZ||, ||XA| \pm |XP| \pm |YZ||, ||YB| \pm |XA| \pm |XP||, ||YB| \pm |XA| \pm |YZ||, ||YB| \pm |XP| \pm |YZ||, ||YB| \pm |XA| \pm |XP| \pm |YZ||\}$,

$|ZR| \notin \{|XS|, |XP|, |XA|, |YB|, ||ZQ| \pm |XP||, ||ZQ| \pm |XS||, ||XP| \pm |XS||, ||YB| \pm |XS||, ||XA| \pm |XS||, ||XA| \pm |YZ||, ||YB| \pm |XA||, ||XS| \pm |YZ||, ||XA| \pm |XS| \pm |YZ||, ||YB| \pm |XA| \pm |XS||, ||YB| \pm |XS| \pm |YZ||, ||YB| \pm |XA| \pm |YZ||, ||YB| \pm |XA| \pm |XS| \pm |YZ||\}$.

By Corollary 4, the union of the two sets of conditions in Lemmas 14 and 15 constitutes a set of sufficient conditions for the line-rigidity of the 6:6 jewel of Fig. 19. Taking care of overlapping conditions between the two sets of conditions, we have 74 distinct conditions for the line-rigidity of the 6:6 jewel and hence the following lemma:

Lemma 16 *The 6:6 jewel $XABYCDPQZRS$ of Fig. 19 is line rigid if its edges satisfy the following conditions:*

1. $|YZ| \notin \{|XA|, |XD|, |XP|, |XS|, ||XA| \pm |XP||, ||XD| \pm |XP||, ||XA| \pm |XS||\}$,

2. $|YB| \notin \{|XA|, |XD|, |XP|, |XS|, ||XA| \pm |XD||, ||XA| \pm |XP||, ||XA| \pm |YZ||, ||XP| \pm |YZ||, ||XS| \pm |YZ||, ||XA| \pm |XS||, ||XA| \pm |XP| \pm |YZ||, ||XA| \pm |XS| \pm |YZ||\}$,

3. $|ZQ| \notin \{|XA|, |XS|, |XD|, |YB|, |XP|, ||XA| \pm |XP||, ||XD| \pm |XP||, ||XA| \pm |YZ||, ||YB| \pm |XA||, ||XD| \pm |YZ||, ||YB| \pm |XP||, ||XP| \pm |XS||, ||XP| \pm |YZ||, ||XA| \pm |XP| \pm |YZ||, ||XD| \pm |XP| \pm |YZ||, ||YB| \pm |XA| \pm |XP||, ||YB| \pm |XA| \pm |YZ||, ||YB| \pm |XP| \pm |YZ||, ||YB| \pm |XA| \pm |XP| \pm |YZ||\}$,

4. $|YC| \notin \{|XD|, |XA|, |XP|, |ZQ|, ||YB| \pm |XA||, ||YB| \pm |XD||, ||XA| \pm |XD||, ||XD| \pm |XP||, ||XD| \pm |YZ||, ||XP| \pm |YZ||, ||ZQ| \pm |XD||, ||ZQ| \pm |XP||, ||YB| \pm |XA| \pm |XD||, ||XD| \pm |XP| \pm |YZ||, ||ZQ| \pm |XD| \pm |XP||, ||ZQ| \pm |XD| \pm |YZ||, ||ZQ| \pm |XP| \pm |YZ||, ||ZQ| \pm |XD| \pm |XP| \pm |YZ||\}$,

5. $|ZR| \notin \{|XS|,\ |XP|,\ |XA|,\ |YB|,\ ||ZQ| \pm |XP||,\ ||ZQ| \pm |XS||,\ ||XP| \pm |XS||,\ ||YB| \pm |XS||,\ ||XA| \pm |XS||,\ ||XA| \pm |YZ||,\ ||YB| \pm |XA||,\ ||XS| \pm |YZ||,\ ||ZQ| \pm |XP| \pm |XS||,\ ||XA| \pm |XS| \pm |YZ||,\ ||YB| \pm |XA| \pm |XS||,\ ||YB| \pm |XS| \pm |YZ||,\ ||YB| \pm |XA| \pm |YZ||,\ ||YB| \pm |XA| \pm |XS| \pm |YZ||\}$.

In the next section we show how a composite *ppg* can be constructed by satisfying all the 74 conditions for each such jewel.

4.3 Algorithm

It is interesting to note that the substitution mechanism has generated rigidity conditions on the strut YZ (Condition 1 of Lemma 16). This implies that, unlike the case for a 5:5 jewel, we will need a pool of nodes, S, for which the pairwise distances of all pairs are known and from which we choose the end nodes of a strut in order to meet the rigidity conditions on YZ. We have to choose the size of S carefully. Since there are 10 conditions on the length of an YZ, from Observation 1 it follows that there must be at most 21 edges incident to the end-node Y, when we are looking for the other end-node Z of a strut.

However, if we use 22 designated nodes for the selection of Z for a particular Y it may happen that all the 6:6 jewels get attached to the same designated node Z. This hinders our goal of obtaining a better value for α than previously known.

Thus, we would like to attach the 6:6 jewels to the designated nodes in such a way that the number of jewels attached to two distinct nodes differ at most by 1. Let the *valence* of a node in this set be the number of times it is used as the end node of a strut to attach a jewel. The following lemma tells us how big S must be.

Lemma 17 *A set S of 42 nodes is sufficient to ensure that the valence of two nodes in S differ by at most 1.*

Proof: To build a 6:6 jewel we set, say Y, to a lowest valence node in S. Of the remaining 41 nodes, at most 20 nodes may not be chosen as Z because of the conditions on YZ (Condition 1 of Lemma 16). From the remaining candidate nodes that satisfy the conditions on YZ we set Z to the one with lowest valence. This way we can attach the first 11 6:6 jewels to 22 fixed nodes that do not have any 6:6 jewel attached to them. Thus, each of these 22 nodes will have valence 1; the rest are of valence 0.

Next we can keep selecting at least 1 node (as Y, say) from the 20 nodes of valence 0 until all are used up. The valence of this 20-node set will be raised to 1. If the second node is not found in that group we can choose it from the other group of valence 1, raising its valence to 2. Now, there is no node of valence 0, at least 22 nodes of valence 1 while the rest are of valence 2. Note that when both

the nodes of a pair are chosen from the set of nodes of valence 0 the number of nodes of valence 1 is increased by 2. Consequently, the number of nodes of valence 1 remains even. When only one node is chosen from the set of nodes of valence 0, there being at least 22 nodes of valence 1 we can choose the other node from this set. This increases the number of nodes of valence 1 by 1 and decreases it by 1 at the same time. Thus, in both the cases there will always be an even number of nodes of valence 1. If there are more than 20 nodes of valence 1 we can choose pairs of nodes for Y and Z from nodes of valence 1 until exactly 20 nodes remain. Eventually, there will be 20 nodes of valence 1 and 22 of valence 2.

We shall show that we can attach the 6:6 jewels in such a way that at any point of time the fixed nodes will have at most 3 consecutive levels of valence. For this we use induction. Let us assume that there are 20 nodes of valence d and 22 nodes of valence $d+1$.

We can choose at least 1 node from valence d nodes and at most 1 node from valence $d+1$ nodes with a total of 2 to form a 6:6 jewel until there is no node of valence d. Then there will be at least 22 nodes of valence $d+1$. The rest are of valence $d+2$. As above we argue similarly to show that there will always be an even number of nodes of valence $d+1$.

If there are more than 20 nodes of valence $d+1$ we can use them in pairs as in the initial round above until the number of degree $d+1$ nodes are exactly 20. The rest 22 will be of degree $d+2$. Now the situation is the same as when we started except that the levels have increased by 1. □

The set S of 42 nodes can be set as the vertices of 8 4:4 jewels hanging from a common strut. Since each 4:4 jewel is line rigid so is this configuration. We will call the nodes in S fixed since we can fix their placement on a line by querying the edges of this *ppg*.

From Condition 2 of Lemma 16 we see that we need 48 extra edges for the selection of an YB that satisfies all the conditions on it as stated in the lemma. Similarly, by Conditions 3, 4 and 5 of Lemma 16 we need 98 extra edges for ZQ, 96 extra edges for YC and 96 extra edges for ZR respectively. Thus, 98 extra edges at Y and Z will suffice to satisfy all the conditions on these edges. In addition to these extra 98 edges we need 2 more edges to accommodate the difference of 1 6:6 jewel that can be attached to them. Thus, we need a total of 100 extra edges at each of the 42 nodes of S.

The main idea underlying the algorithm below is to construct multiple copies of a 6:6 jewel over two rounds to ensure their rigidity. We use the set of nodes S as reference points. Any set of 42 points is chosen as S. The pair of nodes $\{Y, Z\}$ that make up the strut YZ (see Fig. 19) of a 6:6 jewel, is chosen from the set S. As part of the first round, a line rigid layout of S is fixed by attaching eight 4:4 jewels of Fig. 8 from a common strut. The common strut of the 4:4 jewels joins two nodes of S. Pairwise distances of some other suitable nodes are also queried in the first round.

Now we consider the second round. Let $S' = P \setminus S$ be the complement of S. In the second round, the positions of all the nodes of S' are fixed relative

to the nodes in S by first selecting groups of 9 nodes each from S' and placing them relative to a pair of nodes $\{Y, Z\}$ of S. For this, we select a node $Y \in S$ which has the lowest valence of 6:6 jewel of Fig. 19 and a 5-link (X, A, D, P, S). Then we select a node $Z \in S$ such that it has the lowest valence of 6:6 jewel of Fig. 19 and that $|YZ|$ satisfies all the conditions of rigidity on it as stated in Condition 1 of Lemma 16. Thereafter, the nodes B, C, Q and R of S' are selected such that the conditions of rigidity on $|YB|$, $|ZQ|$, $|YC|$ and $|ZR|$ as stated in respectively Conditions 2, 3, 4 and 5 of Lemma 16 are satisfied. Then we query the remaining necessary pairwise edge distances $|AB|, |CD|, |PQ|$ and $|RS|$ of the group to form a 6:6 jewel. The jewel will be line rigid by Lemma 16 irrespective of the lengths of the edges AB, CD, PQ and RS, since no condition of the lemma involves any of these edges. The unused nodes of S' are made line rigid by using 4-cycle as the *ppg*.

Algorithm 2. As in Algorithm 1, we use the following indexing scheme: $X \to X_i$, $A \to A_i$, $B \to B_j$, $C \to B_k$, $D \to D_i$, $P \to P_i$, $Q \to Q_m$, $R \to Q_l$, $S \to S_i$, $Y \to Y_u$ and $Z \to Y_v$.

Let the total number of points be n. We attach b 6:6 jewels (Fig. 19) to each of 20 fixed nodes in S and $b + 1$ to the remaining 22. This gives us a total of $21b + 11$ jewels.

In the first round, we make distance queries represented by the edges of the graph in Fig. 28. All the nodes Y_u $(u = 1, ..., 42)$ (or, Y_v, $v = 1, ..., 42$) in the subgraph enclosed by the rectangle are fixed in the first round by using the 4:4 jewel of Fig. 8 as the *ppg*. There are 8 4:4 jewels (Fig. 8) attached to a common strut, 42 nodes and 65 edges in the subgraph. Each vertex Y_u $(u = 1, ..., 42)$ (or, Y_v, $v = 1, ..., 42$) has $2b+100$ leaves to attach b or $b+1$ 6:6 jewels (Fig. 19). Since there will be $21b + 11$ 6:6 jewels we have $21b + 11$ groups of 5 nodes $(A_i, D_i, S_i, P_i, X_i)$ $(i = 1, ..., 21b + 11)$. We query the distances $|A_iX_i|$, $|D_iX_i|$, $|S_iX_i|$ and $|P_iX_i|$, $(i = 1, ..., 21b + 11)$ in the first round. We will make a total of $168b + 4309$ pairwise distance queries in the first round for the placement of $n = 189b + 4297$ points.

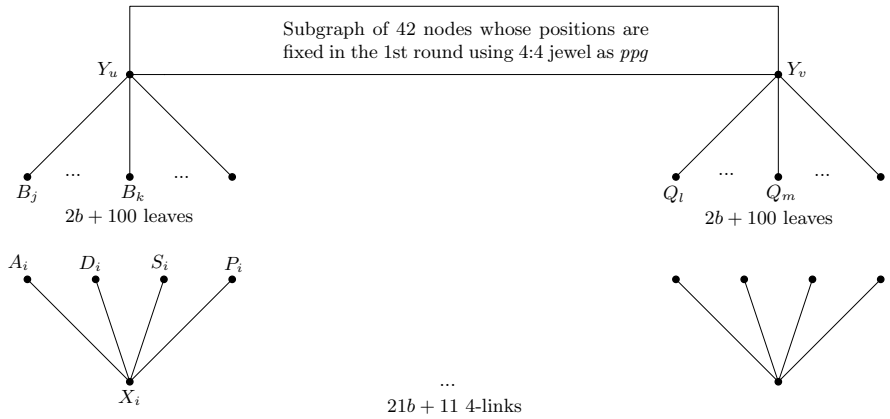

Figure 28: Queries in the first round for 6:6 jewel

In the second round, for each 4-link $(A_i, D_i, S_i, P_i, X_i), i = 1, ..., 21b + 11$, we construct a 6:6 jewel (Fig. 19), satisfying all its rigidity conditions as in Lemma 16. For each such 4-link we select a node Y_u, from the subgraph of 42 fixed nodes $Y_u/Y_v(u, v = 1, ..., 42; u \neq v)$, that has the lowest valency of 6:6 jewel of Fig. 19. Since all the 42 nodes $Y_u, u = 1, ..., 42$, are fixed in the first round, for any pair of such fixed nodes $(Y_u, Y_v)(u, v = 1, ...42; u \neq v)$ we can find the distance $|Y_uY_v|$. So, for each pair of nodes $(Y_u, Y_v)(u, v = 1, ..., 42; u \neq v)$, we shall use (Y_u, Y_v) as an edge in the construction of the 6:6 jewel of Fig. 19. Now from the subgraph of 42 fixed nodes we select another node $Y_v(v \neq u)$ such that the length $|Y_uY_v|$ satisfies all the conditions of rigidity on it as stated in Condition 1 of Lemma 16 and that it has the lowest valency of 6:6 jewel of Fig. 19 among all such qualifying nodes. We note that we can always find such node Y_v, because there will be at most 20 edges Y_uY_v whose length do not satisfy the rigidity conditions on it (Condition 1 of Lemma 16) whereas we have 41 nodes for choosing the node Y_v.

Then we find an edge Y_uB_j rooted at Y_u satisfying the conditions of rigidity on it as stated in Condition 2 of Lemma 16, then we find another edge Y_vQ_m rooted at Y_v satisfying the conditions of rigidity on it as stated in Condition 3 of Lemma 16, then we find another edge Y_uB_k rooted at Y_u satisfying the rigidity conditions on it as stated in Condition 4 of Lemma 16 and, finally, we find another edge Y_vQ_l rooted at Y_v satisfying the rigidity conditions on it as stated in Condition 5 of Lemma 16. Then for each $i, (i = 1, ..., 21b + 11)$, we query the distances $|A_iB_j|$, $|D_iB_k|$, $|S_iQ_l|$ and $|P_iQ_m|$ to form a 6:6 jewel $X_iA_iB_jY_uB_kD_iP_iQ_mY_vQ_lS_i$. Its edges will satisfy all the rigidity conditions of Lemma 16. Thus, all the $21b+11$ 4-links will be consumed to construct $21b+11$ jewels. For this $84b + 44$ edges will be queried.

There will be unused leaves B_j (or Q_l) numbering 100 for each of 20 fixed nodes Y_u $(u = 1, ..., 42)$ (or, Y_v, $v = 1, ..., 42$) and 98 for each of 22 fixed nodes Y_u $(u = 1, ..., 42)$ (or, Y_v, $v = 1, ..., 42$). The total number of such unused nodes is 4156. We use a 4-cycle *ppg* to fix them in the second round. As before, for each pair of nodes $(Y_u, Y_v)(u, v = 1, ..., 42; u \neq v)$, we shall use Y_uY_v as an edge in the construction of the 4-cycle. For each unused node B_j rooted at Y_u we find another node Q_l rooted at Y_v such that $|Y_uB_j| \neq |Y_vQ_l|$. Then the 4-cycle $B_jY_uY_vQ_l$ will be line rigid (Observation 2). Then we query the distance $|B_jQ_l|$ to complete the 4-cycle.

Note that we can always find a node like Q_l. For after repeated selection of such matching pairs of edges there may remain at most 2 edges Y_uB_j rooted at Y_u of length equal to that of the same number of edges rooted at Y_v (Observation 1). In such a situation we switch the matching to match such edges rooted at Y_u with edges other than those same length edge/s rooted at Y_v - this is always possible because there are at most 2 edges rooted at Y_v that have the same length (Observation 1).

For 4156 unused nodes (after the construction of the 6:6 jewel) there will be 2078 4-cycles, and 2078 edges will be queried to complete the 4-cycles. The total number of queries in the second round will be $(84b+44)+2078$, i.e., $84b+2122$.□

Theorem 10 *The ppg constructed by Algorithm 2 is line rigid.*

Proof: The proof is similar to that of Theorem 8 for the line rigidity of the *ppg* constructed by Algorithm 1 and is omitted. □

The number of queries in the first and second rounds are $168b + 4309$ and $84b + 2122$ respectively. Thus, in 2 rounds a total of $252b + 6431$ pairwise distances are to be queried for the placement of $189b + 4297$ points. It is interesting to note that our algorithm would need at least 4486 points to work, which makes it reasonably practical. When we have fewer points we can use Algorithm 1 instead.

Now, $252b + 6431 = (252/189) * (189b + 4297) - (4/3) * 4297 + 6431 = 4n/3 + (19293 - 17188)/3 = 4n/3 + 2105/3$. Thus, we have the following theorem:

Theorem 11 $4n/3 + 2105/3$ *queries are sufficient to place n distinct points on a line in two rounds.*

A consequence of the last theorem is that our 6:6 jewel algorithm is better than the 5-cycle algorithm of Chin *et al.* [4] for $n \geq 11851$.

5 Lower Bound for Two Rounds

In this section we revisit the adversarial argument given by [4] to establish a lower bound on 2-round algorithms. We show that a deeper analysis improves the lower bound substantially.

Let $\mathcal{A}$ denote any 2-round algorithm and $\mathcal{B}$ an adversary. The latter returns a value for the distance between any two points queried by $\mathcal{A}$. $\mathcal{B}$ can also assign value to the distance between a pair of points *not queried* by A. While $\mathcal{A}$'s goal is to make as few distance queries as possible, $\mathcal{B}$ intends to keep the linear placement of the points as ambiguous as possible.

In the *first round*, $\mathcal{A}$ queries the distances between pairs of nodes corresponding to the edges E_1 of the *ppg*, $G_1 = (V, E_1)$. In response, $\mathcal{B}$ returns queried edge-lengths consistent with the following 3-part strategy.

A vertex of degree 3 or more of a *ppg* (in particular G_1) will be called *heavy*.

S1. The placement of all heavy nodes is fixed and the lengths of the edges incident to these nodes are set.

S2. For each node of degree 2 that is connected to a node of degree 1, the length of one of the two edges incident to the degree 2 node is set to a fixed value $c > 0$.

S3. Let $\mathcal{P}_k = p_1, p_2, ..., p_k (k \geq 2)$ be a maximal path of degree 2 nodes, $p_i, i = 1, \ldots, k$; p_0 and p_{k+1} are 2 non-degree 2 nodes adjacent to p_1 and p_k respectively.

First $\mathcal{B}$ sets $|p_{i-1}p_i| = |p_{i+1}p_{i+2}|$ for $i = 1 \pmod 3$.

If both p_0 and p_{k+1} are heavy nodes, then it sets $|p_ip_{i+1}| = |p_{i-1}p_{i+2}|$ for $i = 1 \pmod 3$ and also fixes the layout of the nodes $p_i, i = 0 \pmod 3$.

Otherwise, if at least one of them, say p_{k+1}, is of degree one $\mathcal{B}$ sets $|p_kp_{k+1}| = |p_{k-2}p_{k-1}|$. Also, except for the edges whose length is c, $\mathcal{B}$ sets the lengths of the rest of the edges to lie between $2c$ and $3c$.

Lemma 18 *Strategies S2 and S3 of $\mathcal{B}$ are mutually consistent.*

Proof: Consider a path $\mathcal{P}_k$ of degree 2 nodes in G_1 such that both p_0 and p_{k+1} have degree 1. If $k = 1$, only S2 comes into play and in this case $\mathcal{B}$ sets $|p_1p_2| = c$. For all $k \geq 4$, $\mathcal{B}$ sets $|p_1p_2| = c$, $|p_{k-1}p_k| = c$ in accordance with S2 and the lengths of all other edges in accordance to S3. Figs. 29(c)-29(f) serve as examples of this length assignment since for any k, the total number of edges is a multiple of 3 as in Fig. 29(d), or a multiple of 3 plus 1 as in Fig. 29(e), or a multiple of 3 plus 2 as in Fig. 29(f).

For $k = 2$ and $k = 3$ $\mathcal{B}$ makes the length assignments as shown Figs. 29(a)-(b), which are again consistent with S2 and S3.

If p_0 is heavy, then $\mathcal{B}$ does not have to set $|p_1p_2|$ to c. □

In the *second round*, $\mathcal{A}$ queries the distances between new pairs of nodes corresponding to the edges E_2 of the *ppg*, $G_2 = (V, E_1 \cup E_2)$. In response, $\mathcal{B}$ returns queried edge-lengths consistent with the following strategy:

S4. Let $p_1, p_2, ..., p_k (k \geq 2)$ be a maximal path of degree 2 nodes of length at least 2 in G_1. Let p_0 and p_{k+1} be non-degree 2 nodes adjacent to p_1 and p_k respectively.

If at least one of them, say p_{k+1}, is of degree 1 in the first round and if, for some i with $i = 1 \pmod 3$ and $i < k$, no edge is connected to either p_i or p_{i+1} in the second round by the algorithm then $\mathcal{B}$ sets $|p_ip_{i+1}| = |p_{i-1}p_{i+2}|$ for one of those values of i in the second round.

Or, if no edge is connected to either p_{k-1} or p_k in the second round by $\mathcal{A}$, then $\mathcal{B}$ sets $|p_{k-1}p_k| = |p_{k-2}p_{k+1}|$.

An important observation is in order: the above strategies of $\mathcal{B}$ do not prevent $\mathcal{A}$ from making a linear placement of the vertices of a maximal path of degree 2 nodes that joins a heavy node to a node of degree 1 in distinct positions.

Let p_0 be a heavy node. Consider all the maximal paths $\mathcal{P}_k$ of degree 2 nodes incident to p_0, whose other end is of degree 1. For each path, $\mathcal{B}$ computes the sum of the lengths of all the edges in the path. Let l_{max} be the maximum of all the sums. $\mathcal{B}$ maintains an interval of this length on either side of p_0 free from the placement of the nodes that lie on a path $\mathcal{P}_k$ incident to p_0 whose other end is a heavy node. This is ensured as follows:

1. The distance between p_0 and an adjacent heavy node is at least l_{max}.

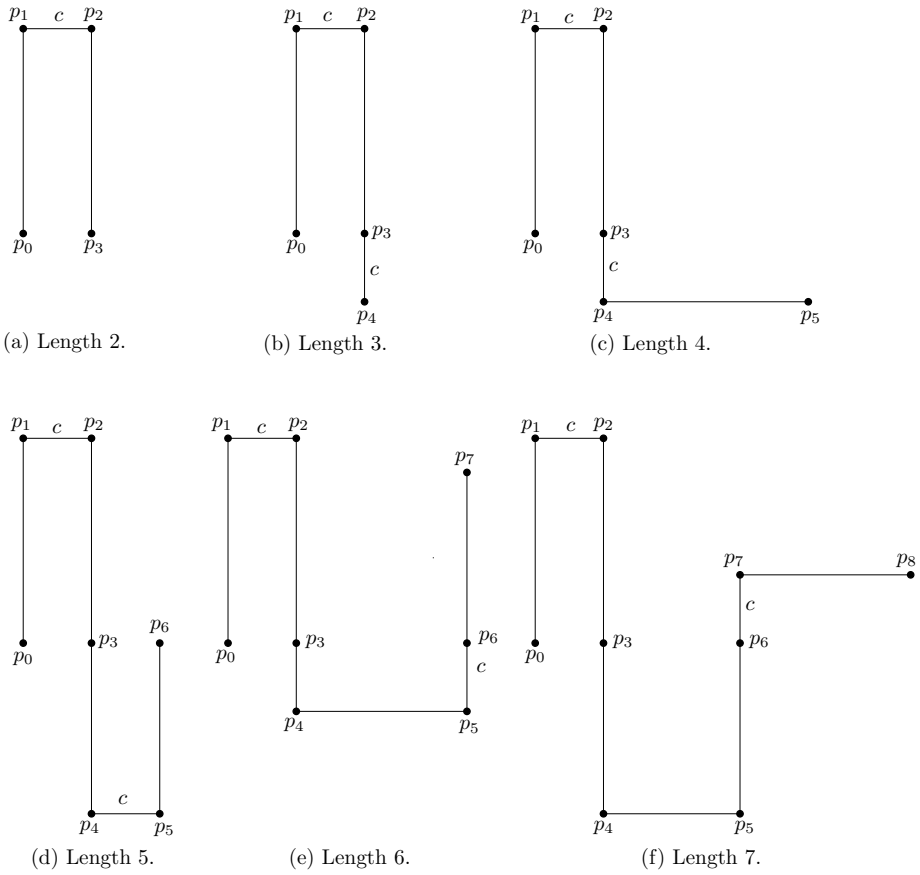

(a) Length 2. (b) Length 3. (c) Length 4.

(d) Length 5. (e) Length 6. (f) Length 7.

Figure 29: The residual parts of maximal paths of degree 2 nodes that will satisfy Step 2

2. Let $\mathcal{P}_k = p_0p_1p_2$. In this case, $\mathcal{B}$ sets $|p_0p_1| > l_{max}$. If $\mathcal{P}_k = p_0p_1...p_{k+1}$, where $k > 1$, $\mathcal{B}$ sets $|p_0p_1| = |p_2p_3| > l_{max}$ and $|p_1p_2| > 2|p_0p_1|$. This ensures that all the vertices of the prefix segment $p_0p_1p_2p_3$ of the path is at a distance farther than l_{max} away from p_0. Clearly the remaining vertices on $\mathcal{P}_k$, however placed, will also be at a distance farther than l_{max}.

The strategies adopted by $\mathcal{B}$ bound the lengths of maximal paths formed by degree 2 nodes in G_2. The precise results are given in the next 3 lemmas.

Lemma 19 *In G_2, the length of a longest chain of consecutive edges from E_1 that terminates on a heavy node at each end of the chain is 4.*

Proof: Let p_0 and p_{k+1} be non-degree 2 nodes adjacent to a maximal path $\mathcal{P}_k = p_1, p_2, ..., p_k$, $(k \geq 4)$, of degree 2 nodes in G_1.

We first consider the case when both of p_0 and p_{k+1} are heavy nodes of G_1. Given strategy S3 of $\mathcal{B}$, if for an $i < k$, with $i = 1 \pmod 3$, $\mathcal{A}$ attaches no edge to either p_i or p_{i+1} in the second round then their positions will be ambiguous (Observation 2). Thus, the lemma is settled for this case.

Consider the case when p_{k+1} is of degree 1. In view of strategies S3 and S4 of $\mathcal{B}$, $\mathcal{A}$ must attach an edge at p_i or p_{i+1} in the second round, for $i < k$ and $i = 1 \pmod 3$, to make the placements of these nodes unambiguous (Observation 2). Thus, the lemma is settled for this case also. □

Lemma 20 *A maximal path $\mathcal{P}_k$ of degree 2 nodes in G_2 that contains at least one edge of E_2 can have at most 2 consecutive edges of E_1.*

Proof: Let $\mathcal{P}_k (k \geq 2)$ be a maximal path of degree 2 nodes in G_1; p_0 and p_{k+1} are non degree 2 nodes adjacent to p_1 and p_k respectively, one of which is of degree 1 in G_1.

Suppose p_0 is of degree 1 in G_1. In view of strategy S3 of $\mathcal{B}$, if no edge is connected to either p_i or p_{i+1} for some $i = 1 \pmod 3$ then following strategy S4, $\mathcal{B}$ will set $|p_i p_{i+1}| = |p_{i-1} p_{i+2}|$ for one of those values of i in the second round. Thus, there must be an edge connected to either p_i or p_{i+1} for all $i = 1 \pmod 3$. In particular, $\mathcal{A}$ must add an edge to be incident to p_1 or p_2 (when $i = 1$).

If p_{k+1} is of degree 1 then following strategy S3 the adversary sets $|p_k p_{k+1}| = |p_{k-2} p_{k-1}|$ in the first round. If $\mathcal{A}$ attaches no edge to either p_{k-1} or p_k in the second round, then following S4, $\mathcal{B}$ sets $|p_{k-1} p_k| = |p_{k-2} p_{k+1}|$. This makes the placements of the nodes p_{k-1} and p_k ambiguous (Observation 2). Thus, $\mathcal{A}$ must attach an edge to p_{k-1} or p_k to preempt $\mathcal{B}$.

Thus, for both the cases, there will be at most 2 nodes of degree at most 2 at an end of a path of degree 2 nodes of G_1, if the end node is of degree 1. The algorithm will place them in the second round by introducing edge/s to one or both of them. Thus, in a maximal path of degree 2 nodes in G_2 that contains at least one edge from E_2 there can be at most 2 consecutive edges from E_1. □

Lemma 21 *The number of nodes in any maximal path of degree 2 nodes in G_2 is at most 3.*

Proof: If a maximal path of degree 2 nodes of G_2 consists of edges from E_1 only then by Lemma 19 its length is at most 3.

Now we consider maximal path of degree 2 nodes of G_2 that contains at least one edge from E_2. In such a path there cannot be three consecutive edges from E_1 (Lemma 20). Suppose the number of degree 2 nodes in such a maximal path is 4. Let the nodes be p_1, p_2, p_3 and p_4. Let p_0 and p_5 be heavy nodes adjacent to p_1 and p_4 respectively. Since any maximal path of degree 2 nodes in G_2 can have at most 2 consecutive edges from E_1 the edges p_0p_1, p_1p_2, p_2p_3, p_3p_4 and p_4p_5 can be from E_1 or E_2 in the following 5 combinations:

1. E_2, E_1, E_2, E_1, E_1
2. E_2, E_1, E_1, E_2, E_1

3. E_1, E_2, E_1, E_2, E_1
4. E_1, E_1, E_2, E_2, E_1
5. E_1, E_1, E_2, E_1, E_1

For combination 1, $\mathcal{B}$ can set the length of the 2 edges in E_2 so that $|p_0p_5| = |p_1p_2| + |p_2p_3|$ and $|p_0p_1| = |p_4p_5| - |p_3p_4|$ (Fig. 30). Then by Theorem 1 the 6-cycle $p_0p_1p_2p_3p_4p_5$ would not be line rigid. Similarly, for the combinations 2-4 $\mathcal{B}$ can make the graph ambiguous. As for combination 5, following S2 $\mathcal{B}$ can set $|p_1p_2| = |p_3p_4| = c$, and can set the length of p_2p_3 in the second round in such a way that $|p_2p_3| = |p_4p_5| + |p_5p_0| + |p_0p_1|$ (Fig. 31). The 6-cycle $p_0p_1p_2p_3p_4p_5$ would not be line rigid then (Theorem 1). □

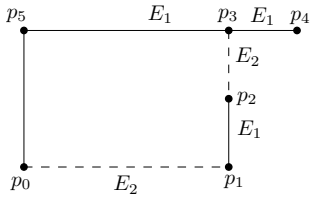

Figure 30: Maximal path of degree 2 nodes in G_2 for the combination of edges E_2, E_1, E_2, E_1, E_1

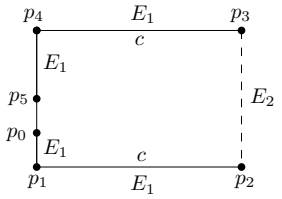

Figure 31: Maximal path of degree 2 nodes in G_2 for the combination of edges E_1, E_1, E_2, E_1, E_1

The *density* of a *ppg*, $G = (V, E)$ is defined as the ratio $|E|/n$, where $n = |V|$. We establish the following lower bound on the density of a *ppg* constructed by any 2-round algorithm.

Theorem 12 *The minimum density of any line rigid ppg for two round queries is at least* 12/11.

Proof: Let each edge of G have weight 1, which we split evenly between the vertices in V that define it. If w_i is the accumulated weight of the i-th vertex, clearly $\sum_{i=1}^{n} w_i = |E|$ so that $n * min_i\{w_i\} \leq |E|$. Thus, $min_i\{w_i\}$ is a lower bound on the density.

We can get a more precise estimate. Observe that a *ppg* has 2 types of nodes, heavy ones (already defined before) and nodes lying on maximal paths of degree 2 nodes that we call *light* nodes. If an edge joins two light nodes or two heavy nodes then the edge weight is divided equally between the nodes. Otherwise, the light node gets $1/2 + g$ of the weight and the heavy node $1/2 - g$ of the weight , where $0 \leq g \leq 1/2$.

The density of a heavy node is at least $3(1/2-g)$. As for light nodes, we note that by Lemma 21 each maximal path of degree 2 nodes has length k, where $k \leq 3$. The total edge weight of such a path is $2(1/2 + g) + (k - 1)$. Thus the average density of each node in such a path is $1 + 2g/k$. It is minimum when $k = 3$. Thus, the density of a light node is at least $1 + 2g/3$.

The minimum average density for all nodes in G_2 is thus

$$\max \min\{3/2 - 3g, 1 + 2g/3\} = 12/11$$

when $g = 3/22$. □

6 Conclusions

It would be quite a challenge to extend this result to 7:7 and 8:8 jewels. The most important contribution of this paper is the improvement to the lower bound for 2-rounds algorithms. Improving this further is a challenging open problem. An interesting direction for further research is to consider learning a set of points on the plane. We are not aware of any published work on this topic.

It might also be interesting to explore the ties of this problem with problems studied under the banner of rigidity theory (see [5, 3]).

References

[1] M. S. Alam and A. Mukhopadhyay. A new algorithm and improved lower bound for point placement on a line in two rounds. In *CCCG '10: Proceedings of the 22nd Canadian Conference on Computational Geometry*, pages 229–232, 2010.

[2] M. S. Alam, A. Mukhopadhyay, and A. Sarker. Generalized jewels and the point placement problem. In *CCCG '09: Proceedings of the 21st Canadian Conference on Computational Geometry*, pages 45–48, 2009.

[3] L. Asimow and B. Roth. The rigidity of graphs. *Trans. Amer. Math. Soc.*, 245:279–289, 1978. doi:10.2307/1998867.

[4] F. Y. L. Chin, H. C. M. Leung, W.-K. Sung, and S.-M. Yiu. The point placement problem on a line - improved bounds for pairwise distance queries. In *Proceedings of the Workshop on Algorithms in Bioinformatics*, volume 4645 of *LNCS*, pages 372–382, 2007. doi:10.1007/978-3-540-74126-8_35.

[5] R. Connelly. Rigidity. In G. P. M. and W. J. M., editors, *Handbook of Convex Geometry*, pages 223–271. 1993.

[6] P. Damaschke. Point placement on the line by distance data. *Discrete Applied Mathematics*, 127(1):53–62, 2003. doi:10.1016/S0166-218X(02)00284-6.

[7] P. Damaschke. Randomized vs. deterministic distance query strategies for point location on the line. *Discrete Applied Mathematics*, 154(3):478–484, 2006. doi:10.1016/j.dam.2005.07.014.

[8] A. Daurat, Y. Gérard, and M. Nivat. The chords' problem. *Theor. Comput. Sci.*, 282(2):319–336, 2002. doi:10.1016/S0304-3975(01)00073-1.

[9] B. Mumey. Probe location in the presence of errors: a problem from DNA mapping. *Discrete Applied Mathematics*, 104(1-3):187–201, 2000. doi:10.1016/S0166-218X(00)00189-X.

[10] J. Redstone and W. L. Ruzzo. Algorithms for a simple point placement problem. In *CIAC'00: Proceedings of the 4th Italian Conference on Algorithms and Complexity*, volume 1767 of *LNCS*, pages 32–43. Springer-Verlag, 2000. doi:10.1007/3-540-46521-9_3.

[11] S. S. Skiena, W. D. Smith, and P. Lemke. Reconstructing sets from interpoint distances (extended abstract). In *SCG '90: Proceedings of the Sixth Annual Symposium on Computational Geometry*, pages 332–339, New York, NY, USA, 1990. ACM. doi:10.1145/98524.98598.

[12] H. Smith and K.W.Wilcox. A restriction enzyme from hemophilus influenzae. i. purification and general properties. *Journal of Molecular Biology*, 51(2):379–391, 1970. doi:10.1016/0022-2836(70)90149-X.